Southeastern Geology: Volume 16, No. 4 May 1975

Edited by: S. Duncan Heron, Jr.

Abstract

Academic journal published quarterly by the Department of Geology, Duke University.

SOUTHEASTERN GEOLOGY

PUBLISHED AT DUKE UNIVERSITY DURHAM, NORTH CAROLINA

VOL. 16 NO. 4 MAY, 1975

SOUTHEASTERN GEOLOGY

PUBLISHED QUARTERLY

AT

DUKE UNIVERSITY

This journal welcomes original papers on all phases of geology, geophysics, and geochemistry as related to the Southeast. Transmit manuscripts to S. DUNCAN HERON, JR., BOX 6665, COLLEGE STATION, DURHAM, NORTH CAROLINA. Please observe the following:

(1) Type the manuscript with double space lines and submit in duplicate.
(2) Cite references and prepare bibliographic lists in accordance with the method found within the pages of this journal.
(3) Submit line drawings and complex tables as finished copy.
(4) Make certain that all photographs are sharp, clear, and of good contrast.
(5) Stratigraphic terminology should abide by the Code of Stratigraphic Nomenclature (AAPG, v. 45, 1961).

Proofs will not be sent authors unless a request to this effect accompanies the manuscript.

Reprints must be ordered prior to publication. Prices are available upon request.

* * * * * *

Subscriptions to Southeastern Geology are $5.00 per volume. Inquiries should be addressed to WM. J. FURBISH, BUSINESS AND CIRCULATION MANAGER, BOX 6665, COLLEGE STATION, DURHAM NORTH CAROLINA. Make check payable to Southeastern Geology.

SOUTHEASTERN GEOLOGY

Table of Contents

Vol. 16. No. 4

May 1975

USE OF ERTS IMAGERY IN THE STUDY OF THE CAPE FEAR PLUME[1]

By

Charles W. Welby
Department of Geosciences
North Carolina State University at Raleigh
Raleigh, North Carolina 27607

ABSTRACT

ERTS-1 imagery has provided the opportunity to study the Cape Fear River plume over a period of more than a year. The suspended material of the waters adjacent to Cape Fear acts as tracers. Dominance of eastward longshore drift west of the river mouth is confirmed, and various patterns of water movement offshore are recorded on the imagery. On two occasions the imagery recorded the existence of a counterclockwise swirl which apparently carried water west of the river mouth first seaward and then back toward Smith Island.

INTRODUCTION

Launched in July, 1972, the Earth Resources Technology Satellite (ERTS-1) has provided repetitive synoptic images of the United States ever since. A wide variety of uses for the data has been described (NASA, 1973), but one of the most promising uses has been the monitoring of coastal processes. The synoptic view afforded by the imagery from the satellite shows suspended sediment distribution in coastal areas, and where the water is shoal enough, there are probably recorded on the imagery patterns of sediment transport at or near the bottom.

A multispectral scanner aboard the satellite records reflections in four bands of the electromagnetic spectrum (500-600 nm; 600-700 nm; 700-800 nm; 800-1100 nm; Bands 4, 5, 6, and 7 respectively). The data received from the satellite can then be studied and interpreted for various purposes. Because of differences in depth penetration of the various parts of the spectrum it is possible to study the vertical distribution of suspended material in coastal waters. Even without

[1]The work described here was done with the support of Goddard Space Flight Center, NASA Contract NAS5-21732.

groundtruth one can develop an improved understanding of certain coastal processes from the ERTS-1 imagery, for suspended materials can act as markers. Their distribution records the currents and water movement.

Correlation of distribution patterns seen on the imagery with wind, tidal, and other appropriate data gives insight to coastal processes. In addition, the repetitive 18-day cycle of ERTS-1 enables those interested in coastal processes to view a particular area responding to a variety of conditions.

The Cape Fear region was chosen for the study as a number of phenomena are recorded on the ERTS-1 imagery of this part of coastal North Carolina. Behavior of the coastal waters is described in the following discussion to provide insight on how suspended sediment in the vicinity of the mouth of the Cape Fear River can move. Also, this area is of interest because of the planned warm water discharge from a nuclear power generating plant of over 2000 cfs at a point 0.4 miles offshore and about 2 miles west of the mouth of the Cape Fear River.

TECHNIQUES

The imagery has been studied in the form of black and white transparencies at various scales up to 1:125,000. For a better understanding of vertical sediment distribution and of variations within the plumes and water masses, color additive viewing and density slicing techniques were used. Minimal groundtruth makes possible quantitative interpretations of the imagery, but important qualitative and semi-quantitative interpretations can often be made without groundtruth. However, the cost of obtaining the information must be weighed against the availability of funds and the needs for the more detailed information.

DISCUSSION

Langfelder et al (1968) have described littoral drift along the North Carolina coast, and Figure 1 summarizes the results of this study for the Cape Fear region. Rudolfo, Buss, and Pilkey (1971) described the effects of a hurricane on the suspended load in the Cape Lookout area, noting the stirring of the bottom at the inshore locations especially and a general increase of suspended material from the surface to the bottom. Prestorm concentrations of suspended material at the surface ranged from 0.5 within 2 km of shore to between 0.2 and 0.3 mg/L out to 20 km offshore. After the storm surface values of suspended sediment were 0.7 mg/L at 2 km and over 2 mg/L 10 km offshore.

Manheim, Meade, and Bond (1970) in their description of the suspended particulate matter of Atlantic continental surface waters show at Cape Fear (Figure 1) that the total suspended matter drops from 4.0

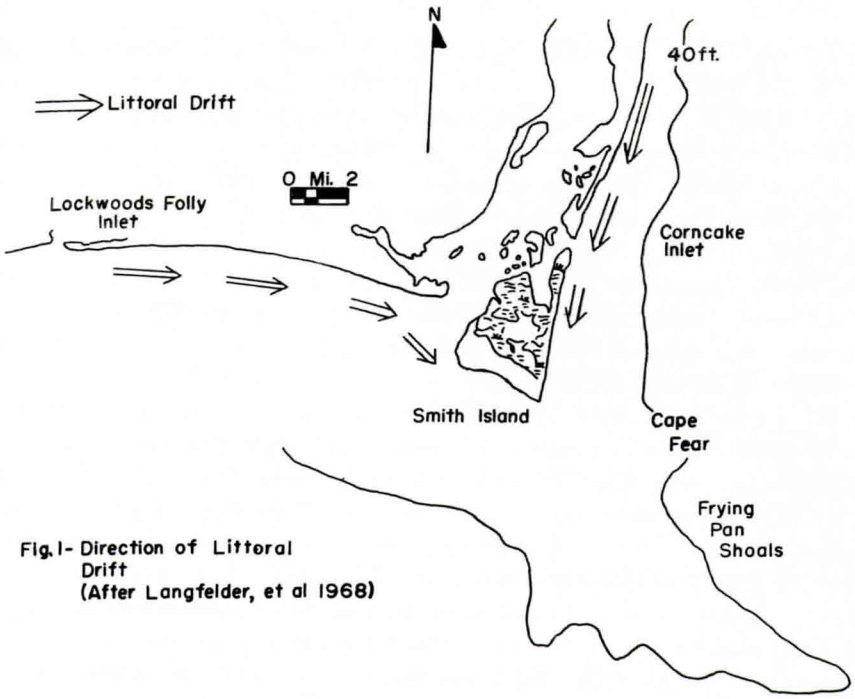

Figure 1. Direction of littoral drift (after Langfelder et al, 1968).

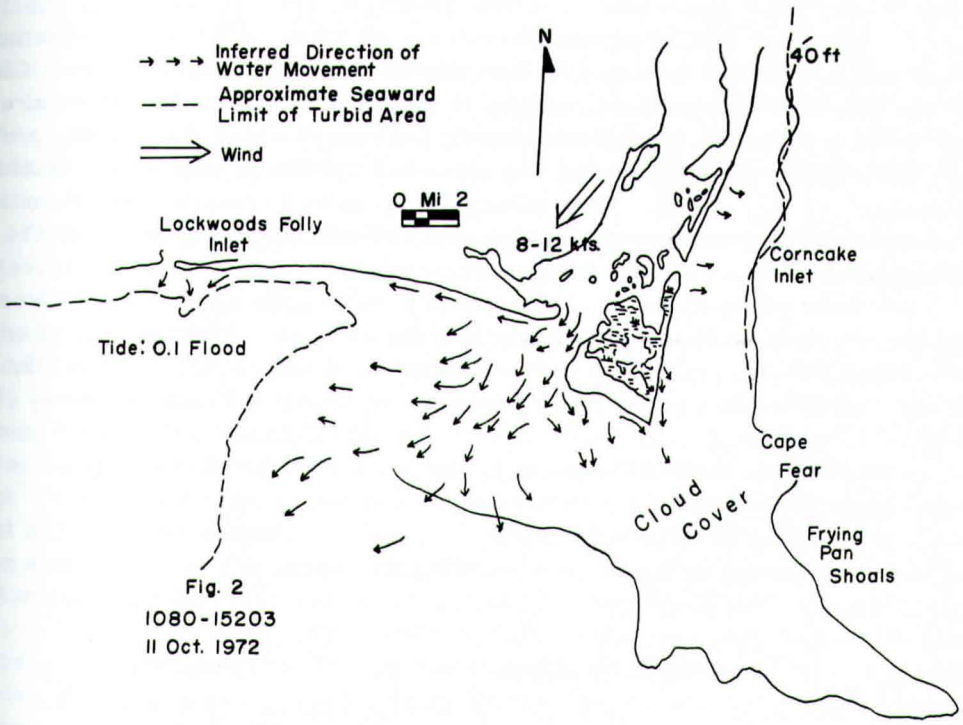

Figure 2. 1080-15203, 11 Oct., 1972.

mg/L near the shore to less than 0.125 mg/L about 30 km offshore. Wide spacing of the sampling points precludes the description of the details of the behavior of the water masses containing the suspended materials. The information is truly valid only for the instant of sampling, although the data probably fairly represent conditions present at the sampling point for some period of time. The study showed that on a rough basis water which contained 1 mg/L or more of suspended material appeared greenish, and that with increasing concentrations of suspended material water became yellowish brown and then reddish brown. No values for the concentrations at which the color changes seemed to occur were noted.

The published information can be used as a guide to the probable concentrations of suspended material found in the waters adjacent to Cape Fear, and the ERTS-1 imagery interpreted on this basis. Since patterns of water movement as shown by the ERTS-1 imagery are the primary interest in this discussion, the load of suspended material need only be measured relatively.

Light penetration into water varies with concentration of suspended materials as well as with the wavelength of the light. It seems probable that light reflected from depths no greater than 10 meters is recorded in the imagery of coastal North Carolina, a conclusion based on experiments elsewhere (Science Engineering Research Group, 1971; Gross, 1972), and it is probable that penetration is somewhat less. Reflections from the very shallow areas are probably recorded in the imagery as they often are in aerial photography.

Figures 2 to 12 show the interpretations of the ERTS-1 imagery. Wind and tidal data are given for the various images. Work in Chesapeake Bay has shown that changes in tide and wind direction are soon followed by changes in the patterns of the suspended materials, reflecting the rapid response of the water to the tidal and atmospheric changes (Bowker et al, 1973). Therefore, it is believed that the patterns recorded by the images generally reflect conditions existing at the time of the pass and for only a short time before.

Table 1 provides data on the flow in the Cape Fear River at a point 65 miles upstream. River flow data are given for the day preceding the imagery also, although tidal action prevents estimation of the time it takes the water passing Lock 1 to reach the mouth of the river (N. O. Thomas, personal communication). Wind and tidal data are shown on each figure; the wind data were obtained from the National Weather Service maps.

Arrows on the figures depict the directions in which the turbid water is inferred to have been moving at the time the image was made. Undoubtedly, the dispersal of the turbid water recorded by the imagery has occurred over several tidal cycles. The materials most recently brought to the mouth of the Cape Fear River or most recently placed in suspension along the shore record on the respective image the most recent nearshore dynamics. In general, concentrations of suspended

Table 1. Discharge on Cape Fear River, at Lock 1 (U. S. G. S.)

Date	Discharge (cfs)	Date	Discharge (cfs)
10 Oct. 1972	4270	1 June 1973	11,800
11 Oct. 1972	3140	2 June 1973	8910
3 Dec. 1972	8600	25 July 1973	4980
4 Dec. 1972	7750	26 July 1973	6150
26 Jan. 1973	13,700	10 Nov. 1973	874
27 Jan. 1973	11,000	11 Nov. 1973	866
21 March 1973	12,400	28 Nov. 1973	1108
22 March 1973	9970	29 Nov. 1973	1100
26 April 1973	4200	21 Jan. 1974	2440
27 April 1973	4460	22 Jan. 1974	2440

material decrease seaward, lines of equal concentration being oriented at right angles to the axes of the arrows.

Image 1080-15203; 11 October 1972 (Figure 2)

Suspended materials occur as a narrow band close to shore north of Cape Fear as well as in irregularly distributed patches along the westward-trending coast, west of the Cape. The most prominent protrusions of suspended material are from the inlets. A narrow band of relatively clear water extends southwesterly from the west end of Smith Island, occurring between the two sets of parallel arrows in Figure 2. It is interpreted as the locus of a major seaward flow of non-turbid water, or a mixing zone between two more turbid water masses where the turbid water is sinking from either side. Alternatively, this feature could represent an area of upwelling.

The imagery points to a general diffusion of the suspended material both in a southwesterly direction and a south-southeasterly direction across Frying Pan Shoals. The plumes at the mouth of the Cape Fear River bulges seaward along a southwestward-trending axis as indicated by the arrows. At the moment of imaging the currents were probably about 2 knots in a seaward direction, the tide having just turned from ebb toward flood.

Band 4 imagery shows a more diffuse pattern southeast of the Cape Fear River with about the same reflectivity pattern along the shore west of the river mouth. Longshore drift seems to have been westward from the mouth of the river. Evidence for this phenomena is recorded in Bands 4, 5, and 6.

Image 1134-15211; 4 December 1972 (Figure 3)

The December 4, 1972, image was taken shortly after the turn

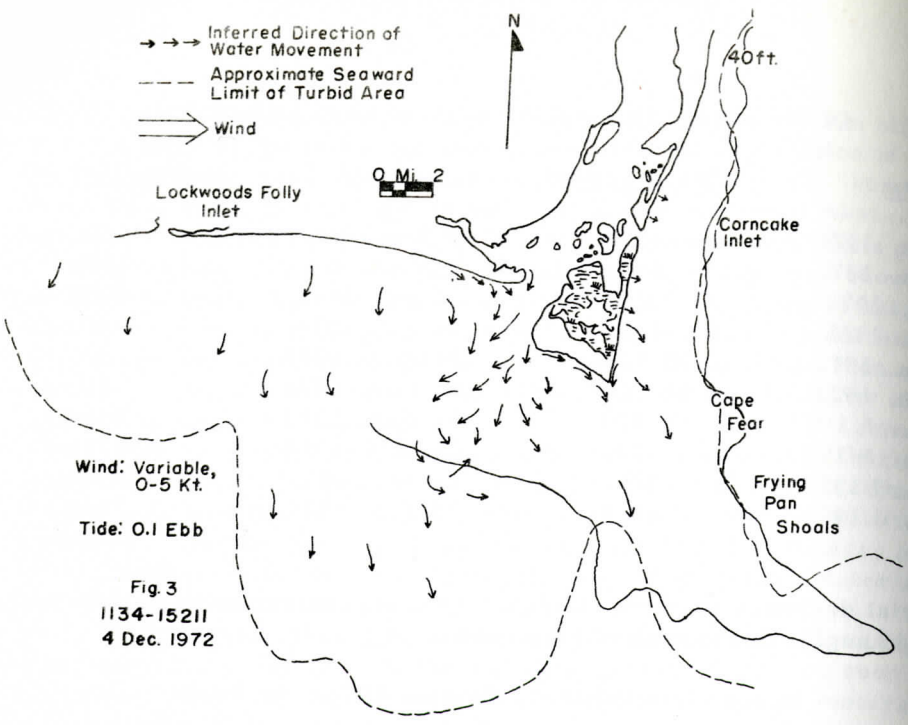

Figure 3. 1134-15211, 4 Dec., 1972.

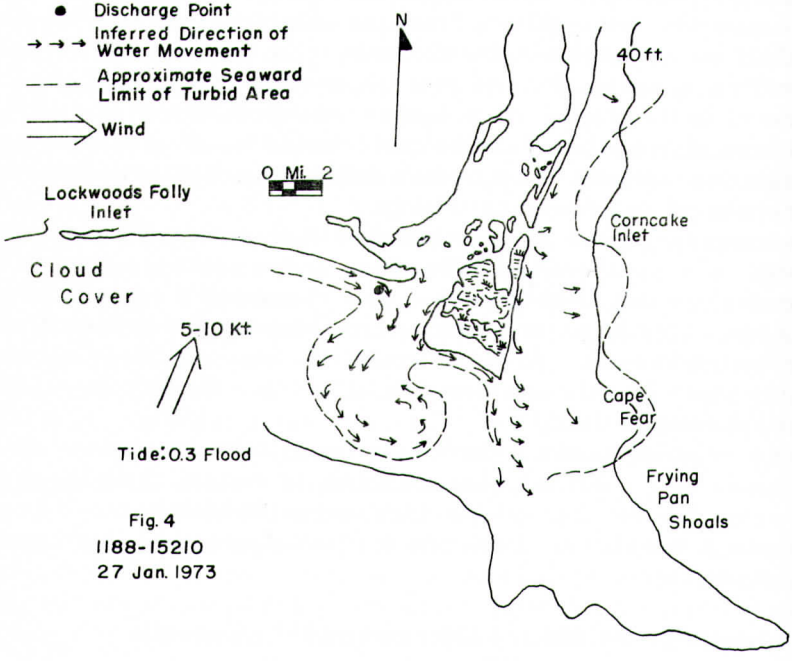

Figure 4. 1188-15210, 27 Jan., 1973.

of the tide from flood to ebb, and currents had reached approximately 0.6 knot downstream. The winds were generally less than 5 knots and variable almost up to the time of passage of ERTS-1. At the time of the pass the winds were blowing at about 5 knots in a southeasterly direction. Figure 3 summarizes the results of the study of this image. Density slices as well as the black and white transparencies show the Cape Fear River discharging water of lower turbidity as a well-defined jet-like feature a few hundred yards west of Smith Island. Adjacent to this particular feature are narrow bands of water with greater turbidity, the eastern one extending to the western end of Smith Island. This relationship is in contradistinction to the pattern seen in the October 11 image where the main channel appears to contain water with greater turbidity, and a band of clear water extends outward from Smith Island.

Instead of being, as might be expected, delta-shaped or bulbous with its apex located at the mouth of the Cape Fear River, the pattern of turbid water is triangular-shaped with the apex about 4 miles south-southwest of the river mouth. The base extends along the shore zone from Cape Fear westward to a position about 2 miles west of the river. Frying Pan Shoals is connected to a narrow belt of high reflectivity close to the shore north of the Cape.

The patterns found on the imagery suggest easterly drift for the water and its accompanying suspended materials. Because the wind had been low in velocity and variable in direction for some time, the pattern probably reflects phenomena that occurred somewhat before the passage of the satellite.

Image 1188-15210; 27 January 1973 (Figure 4)

Cloud cover obscures much of the area adjacent to Cape Fear, but the image shows a bulbous plume approximately 4 miles in diameter extending seaward from the mouth of the Cape Fear River. The internal structure of the plume indicates that the water moved in the counter-clockwise swirl. The path followed by the water leaving the mouth of the Cape Fear River appears to be first to the southwest. About 5 miles offshore the water turned counterclockwise and began to hook toward Cape Fear and continued in a swirl-like pattern.

Winds had been blowing from the south-southwest at less than 10 knots prior to the imaging, and the tide was well toward the flood stage. Currents were moving approximately 0.03 knot in an upstream direction. It appears that the change from ebb to flood tide had not yet affected the bulbous form of the plume. Shown on Figure 4 is the approximate location of the discharge point for the nuclear power generating plant located at Southport.

Image 1242-15213; 22 March 1973 (Figure 5)

The next usable image of the Cape Fear area was made on March

22, 1973. It shows a general diffusion of suspended material with patches of relatively clear water off Carolina Beach. All of Band 4 records the general diffussion of suspended material over Frying Pan Shoals with a northeast-southwest grain or ribbing consisting of alternating bands of greater and lesser concentrations of suspended load. This pattern extends across Frying Pan Shoals out to about eight miles offshore.

Comparison of this image with the earlier images shows that a more diffuse pattern of suspended sediment existed in March than at the earlier times. Also, the suspended sediment load was less at the time of the March image.

Image 1278-15215; 27 April 1973 (Figure 6)

Cape Fear does not appear on this image, but information about adjacent areas is supplied by it. The general diffusion of suspended material north of Cape Fear is modified by a clear band trending north-south located approximately along the 40-foot isobath. This band extends approximately to the latitude of Corn Cake Inlet. Northwestward-trending ragged fingers of suspended material are found in this area also. The seaward boundary of the suspended material is recorded near the mouth of the Cape Fear River and offshore. A band of relatively clear water along the west side of the Cape Fear River is shown by the image. This feature is probably the main channel of the river.

The wind had been blowing eastward at velocities of up to 15 knots prior to the satellite pass. At Cape Fear the tide was about 0.25 of the way to flood, and current velocity was about 0.2 knot in the ebb direction.

The interpretation placed upon the image is that there was a general current movement to the north and northeast north of Cape Fear with swirls developing offshore in a northeasterly direction. Since the patterns are seen better in Band 4 than in Band 5, the implication is that the recorded current movement extended to a significant depth.

Immediately west of the mouth of the Cape Fear the longshore currents were westerly. However, they appear to have encountered an easterly drift about 1.5 miles west of the mouth of the river, and a complex water movement pattern had developed.

Image 1314-15210; 2 June 1973 (Figure 7)

Unlike most of the other images of the Cape Fear area this one shows the presence of a high concentration of reflective material in Bands 6 and 7 (infrared) as well as Bands 4 and 5. The reflectances are present offshore as well as within the Cape Fear River south of Wilmington. For some time prior to the passage of the satellite the winds had been variable in direction from 0 to 5 knots. At the time of the imagery, the tide was ebbing with a current velocity of somewhere near 0.02 knot seaward.

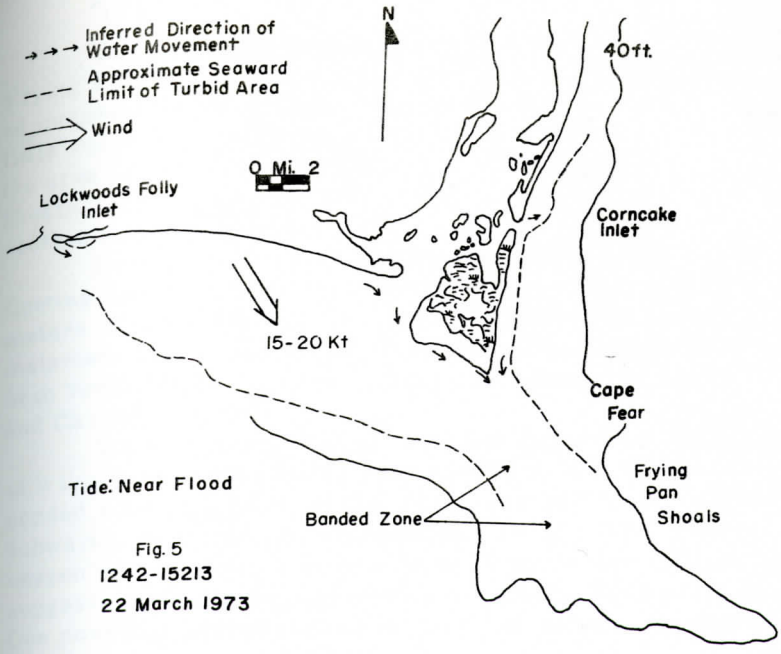

Figure 5. 1242-15213, 22 March, 1973.

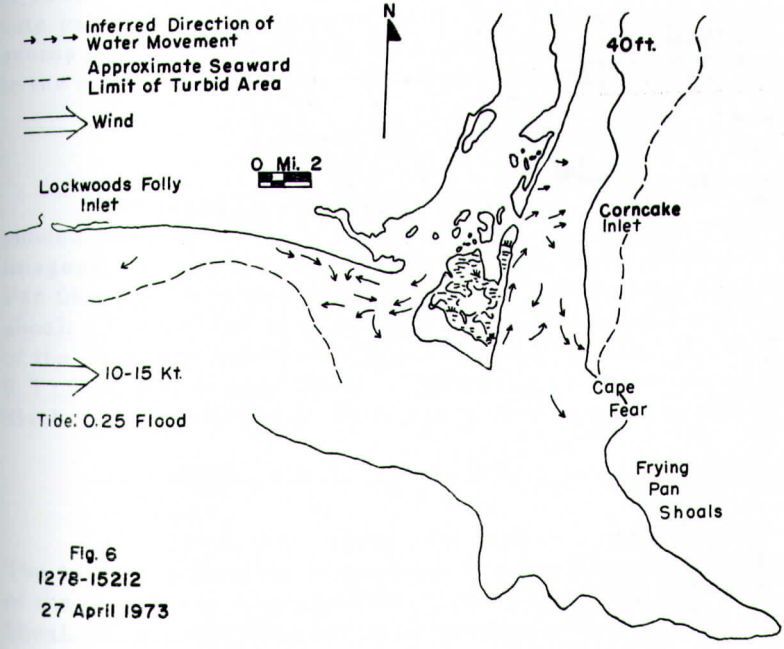

Figure 6. 1278-15212. 27 April, 1973.

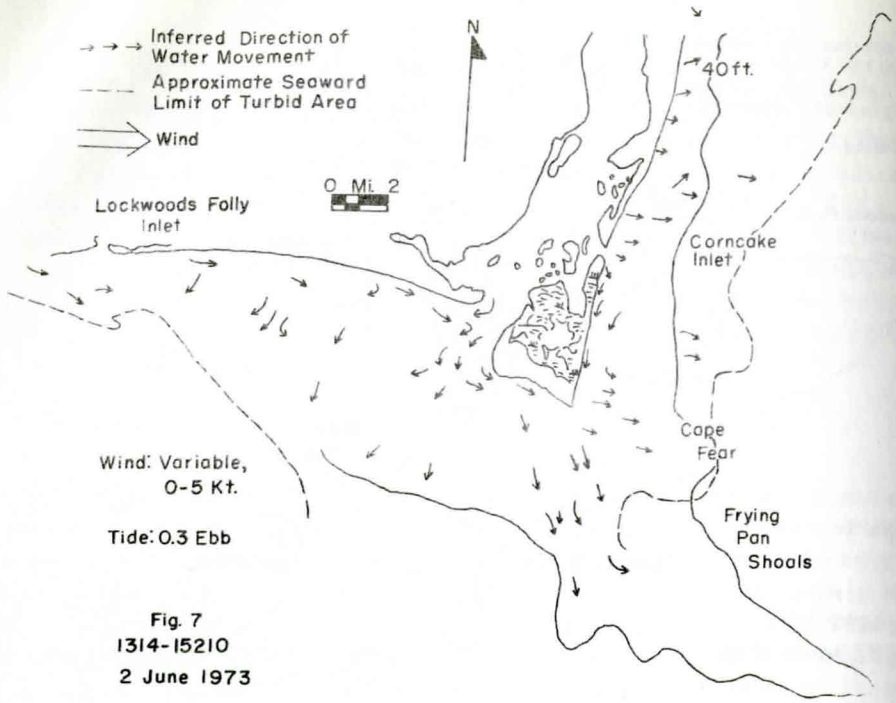

Figure 7. 1314-15210, 2 June, 1973.

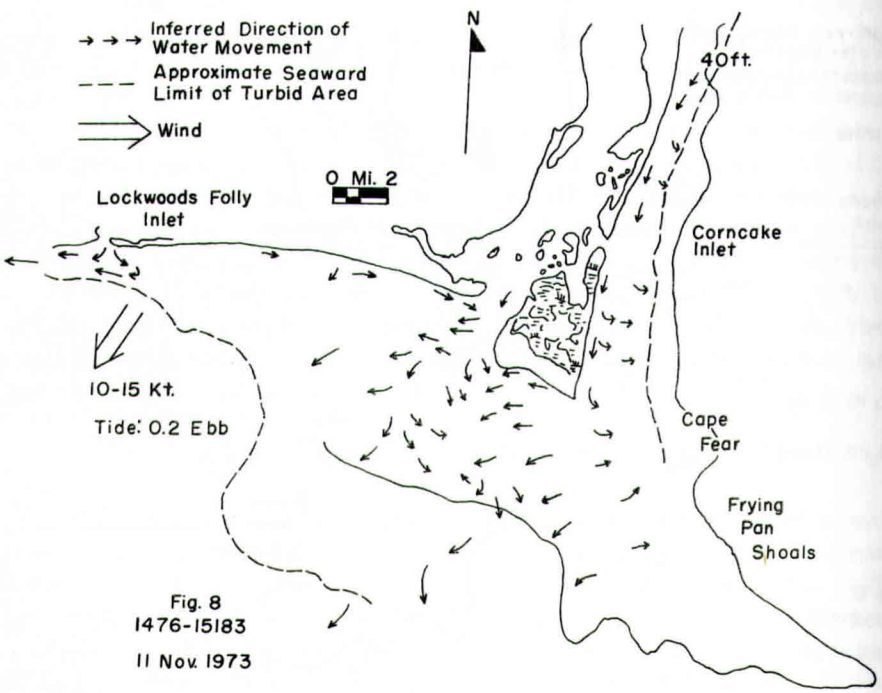

Figure 8. 1476-15183, 11 November, 1973.

The materials suspended in the water has a diffuse pattern over Frying Pan Shoals and north of Cape Fear. Within the area of suspended material north of Cape Fear are several linear areas containing little suspended material. There is a sharp southwesterly boundary to the area of suspended material a short distance west of Frying Pan Shoals. Its approximate boundary is marked on Figure 7 by the south-southeast trending arrows.

Presence of the reflectance in Bands 6 and 7 implies that the reflecting material is on the surface of the water or within just a few millimeters of the surface. The infrared reflection suggests that suspended materials are in large part phytoplankton. Phytoplankton blooms have been recorded on ERTS-1 imagery in Albemarle Sound (Welby, Lammi, and Carson, 1973).

Water quality studies carried out on the Cape Fear River south of Wilmington in the latter part of May prior to the satellite pass recorded a notable drop in the dissolved oxygen content of the water (F. Schwartz, personal communication, 1973). The change in dissolved oxygen content from a normal 8 to 10 parts per million to about 2 ppm suggests strongly that there was an intensification of organic activity. One possible interpretation is that an extensive unrecognized phytoplankton bloom was underway.

Since the same type of reflectances are present north of Cape Fear, the conclusion that a phytoplankton bloom was present there also is reasonable. Density slicing of Band 6 of this image shows an intricate pattern of reflectances north of Cape Fear reminiscent of thin scums of algae irregularly distributed across a pond. lending credence to the conclusion that the reflections are coming from phytoplankton.

Image 1368-15202: 26 July 1973

Compared to the images described previously, much less suspended material is recorded in the waters off Cape Fear on the July 26 imagery. Current activity had stirred up some sediment across Frying Pan Shoals, for wisps and blotches of lighter tone appear crossing the shoal. The pattern suggests a dripping effect and a gradual dispersion of the sediment seaward. The tide had just turned and was less than 0.1 of the way toward flood. The ebbing current was about 0.7 knot. Slack water occurred a little more than an hour after the satellite pass.

Image 1476-15183, 11 November 1973 (Figure 8)

This November image records a complex dispersion pattern. The two most striking phenomena are the eastward longshore drift west of the Cape Fear River and the movement of the water over Frying Pan Shoal. The suspended sediment pattern over the shoal suggests that the water is moving both to the east and west off the shoals in contrast to other instances in which the movement of the water is southeastward

along the axis of the shoal. Extending south-southeastward from the west end of Smith Island, a belt of lower reflectances can be observed on Band 5 imagery. In Figure 8 the belt is marked by the oppositely pointing arrows bordering it. The belt is interpreted as the locus along which oppositely flowing turbid water is sinking. Other images, notably image 1080-15203 (Figure 2) show a belt of relatively clear water extending southward from the same general position.

Image 1494-15182; 29 November 1973 (Figure 9)

The wind had been blowing for several hours at 10 to 20 knots from the northwest prior to the passage of ERTS-1 on 29 November 1973. An eastward drift from Lockwood's Folly Inlet appears to reflect this fact. Turbid water was spilling across Frying Pan Shoals between 1.5 and 2 miles south of Cape Fear, and water was also moving southward along the western edge of the shoals. North of the Cape there was some southward longshore drift close inshore. Seaward, turbid water moved eastward and northeastward.

Image 1548-15170; 22 January 1974 (Figure 10)

Detailed study of the plume shown at the mouth of the Cape Fear River reveals an internal structure which implies a counterclockwise rotation water within the plume. Water from the point at which the plume's western edge encountered the shore near the Oak Island bridge eventually circulates counterclockwise and comes into shore again near the center of Smith Island. The image also suggests that the water may move from the locality near the center of Smith Island diagonally southeastward toward Frying Pan Shoals. Figure 10 illustrates the circulation pattern as interpreted from the image. The tide was approximately 0.6 towards full ebb, and the current velocity was about 1.3 knots in the ebb direction of Smith Island. A similar, though not identical pattern, is recorded by image 1188-15210 of January 27, 1973.

On January 21, 1974, the day before the pass of the satellite, a cold front had passed through the Wilmington area, and winds as high as 20 knots blew from the south and southwest. At the time of the January 22 satellite pass the Cape Fear area lay between two small high pressure cells, and the winds were light and variable. It appears, then, that a circulation pattern off Cape Fear may be reflecting in part the effects of the wind activity of the preceding day.

CONCLUSIONS

ERTS-1 imagery has provided the opportunity to study the behavior of turbid coastal waters in the vicinity of Cape Fear. Under some conditions the longshore drift is eastward west of the Cape Fear

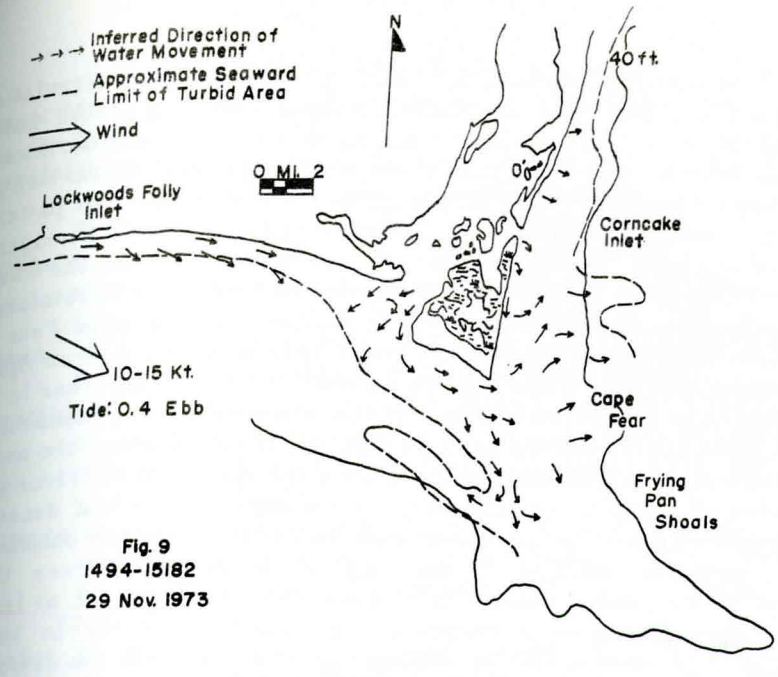

Figure 9. 1494-15182, 29 November 1973.

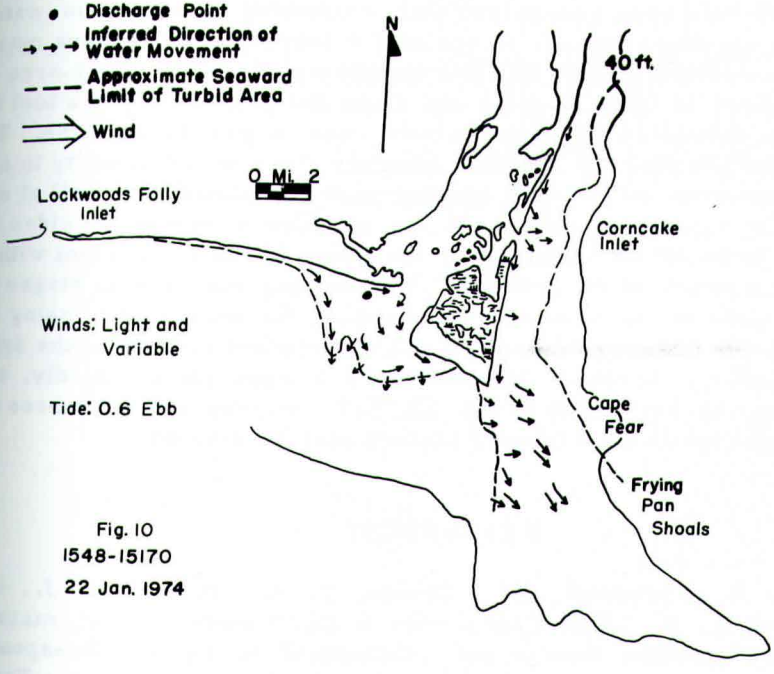

Figure 10. 1548-15170. 22 January, 1974.

River; under others it is west. On at least two occasions the circulation pattern within the plume was counterclockwise, bringing turbid water from west of the mouth of the Cape Fear River eastward and northward toward Smith Island. On other occasions a more general dispersion of the turbid water occurred. The dominant easterly littoral drift pattern described by Landfelder et al (1968) is confirmed by the ERTS imagery. However, the imagery has provided an opportunity to study the water circulation over a much larger area than has been possible heretofore.

Observations made during aircraft flights over the Cape Fear at various times, as well as study of color IR photography taken on April 28, 1973, shows that the water at the mouth of the Cape Fear is in general greenish to yellowish brown. If the observations of Manheim, Meade, and Bond (1971) can be used as a guide, it appears that the average concentration of suspended material near the mouth of the river will be of the order of 2 mg/L or greater. Consideration of the density slicing information leads to the conclusion that at the seaward boundary of the turbid water as marked on the maps of the several figures the concentration of suspended matter is of the order of 0.25 mg/L or less.

If the drop in dissolved oxygen in the Cape Fear River in May and June of 1973 is attributable to biological activity, then the usefulness of the imagery for monitoring phytoplankton blooms in the coastal waters of North Carolina has been demonstrated, for image 1314-15210 clearly records a surface phenomenon in the infrared band.

It has long been recognized that suspended material in water provides an excellent marker or tracer for movement of various masses. The availability of the ERTS-1 imagery of the Cape Fear area as well as the area of Cape Lookout and Cape Hatteras provides a tool for studying the dynamics of these areas over a period of time. The synpotic view afforded by ERTS-1 imagery gives an opportunity to see a whole circulation cell or the greater part of a circulation cell at one instant. The repetitive nature of the satellite coverage provides an opportunity to study the changes in the dynamics of the system within the time framework of the imaging. We can thus see several stages for several patterns of the plume by interpreting the imagery and using it. Admittedly, the imagery does not give the complete picture of the dynamics of the plume because the situations change rather rapidly, and even with the 18-day cycle of the ERTS-1 imagery only glimpses or frames from a continuous moving picture may be studied.

REFERENCES

Bowker, D. E., Fleischer, P., Gosink, T. A., Hanna, W. J., and Ludwick, J., 1973, Correlation of ERTS multispectral imagery with suspended matter and chlorophyll in Lower Chesapeake Bay: Symposium on Significant Results obtained from the Earth Resources Technology Satellite-1, Goddard Space Flight Center,

v. 1, paper M-4, p. 1291-1295.

Goss, M. G., 1972, Oceanography: Prentice Hall, Inc., Englewood Cliffs, N. J., 581 p.

Langfelder, L. J., Stafford, D., and Amein, M., 1968, A reconnaissance of coastal erosion in North Carolina: Department of Civil Engineering, N. C. State University, Project ERD-238.

Manheim, F. T., Meade, R. H., and Bond, G. C., 1970, Suspended matter in surface waters of the Atlantic continental margin from Cape Cod to the Florida Keys: Science, v. 167, p. 371-376.

NASA, 1973, Symposium on significant results obtained from the Earth Resources Technology Satellite: NASA SP-327.

Rudolfo, K. S., Buss, B. A., and Pilkey, O. N., 1971, Suspended sediment increase due to Hurricane Gerda in continental shelf waters off Cape Lookout, North Carolina: Jour. Sed. Petrology, v. 41, p. 1121-1125.

Science Engineering Research Group, 1971, Multispectral photographic remote sensing of coastal environments: Tech. Report, Ser. 6 TR-11, Long Island University C. W. Post Center, Greenvale, NY.

Welby, C. W., Lammi, J. O., and Carson, R. J. III, 1973, Utilization of ERTS-1 data in North Carolina: NASA - CR - 132199. NTIS E73-10688.

LOW-TIDE STORM EROSION IN A SALT MARSH

By

J. Lee Settlemyre
and
L. R. Gardner
Department of Geology and
Belle W. Baruch Coastal Research Institute
University of South Carolina
Columbia, South Carolina 29208

ABSTRACT

This study describes the flood hydrograph and sediment discharge resulting from brief storms occuring during low tide on two small salt marsh drainage basins. The measured values of sediment export resulting from low-tide storm erosion were used to estimate annual sediment yields ranging from 4.3×10^{-2} gm/cm^2/yr to 1.13×10^{-2} gm/cm^{2}yr. Our estimates of annual low-tide storm erosion represent approximately 10-30 percent of the sedimentation rate, 0.13 gm/cm^2, required for vertical marsh growth to keep pace with sea level rise (0.15 cm/yr-Shepard, 1964; Stuiver and Daddario, 1963). Thus, the magnitude of our estimates indicates that the erosion of salt marshes during low-tide storms may be an important component of marsh sediment budgets.

Observations of turbidity, salinity and discharge indicate that the processes of runoff and erosion during such storms involves the following sequence: (1) an initial erosional episode resulting from channel bank runoff and erosion, (2) a runoff peak resulting from the convergence and accumulation of rainfall from the marsh surface into the tidal creek channels, and (3) a salinity minimum owning to the mixing of fresh rain with saline tidal creek water. The observed similarity of these processes in the two drainage basins is a reflection of the similarity in salt marsh basin geometry.

INTRODUCTION

In the course of a long-term study of the chemical quality of runoff from marshlands during low tide, we have observed that large quantities of sediment were exported from small tidal creek basins during rainstorms occurring while the marsh is exposed. On two occasions we had an opportunity to carefully monitor the flow and suspended sediment load of two small creeks during short, low-tide rain squalls.

The measurements obtained were used to estimate annual amounts of exported sediment due to low-tide storm erosion. The results indicate that erosion owing to low-tide storms may be an important component of marsh sediment budgets.

In addition, this report shows that careful measurement of the discharge, salinity and suspended sediment of the runoff provides insight into the processes of runoff and erosion resulting from such events.

Acknowledgments

This is contribution number 120 of the Belle W. Baruch Coastal Research Institute, University of South Carolina. Funds for this study were provided by grants from the Office of Water Resources Research, Department of the Interior, and S. C. Water Resources Research Institute, Clemson University, under Project Number B-055-SC. The authors thank Drs. W. E. Sharp, J. M. Dean, and B. Kjerfve for their helpful review of the manuscript.

DESCRIPTION OF STUDY

Measurements for this study were made at the mouths of two small tidal creeks, one draining the marshlands of the Bellefield Plantation near North Inlet, Georgetown County, South Carolina and the other on the perimeter of the Charleston Harbor estuary, South Carolina. The drainage basin areas for the Bellefield and Charleston tidal creeks, as determined from aerial photographs, are respectively $1.7 \times 10^4 m^2$ and $2.8 \times 10^4 m^2$. The dominant vegetation of the basins is Spartina alterniflora. The semidiurnal tidal range at these locations is 1.5m-1.8m (National Ocean Survey). Neither basin receives drainage from upland areas.

Discharge was measured by means of a right angle notch sheet metal weir (Powell, 1951) emplaced in the beds of the creeks. At the Bellefield creek, the elevation of the weir notch was about 20cm above mean low tide so that discharge could be measured from approximately two hours before to two hours after low water. The elevation of the weir in the Charleston creek was somewhat lower and the period of exposure was generally one to two hours.

Suspended sediment was measured gravimetrically by filtration of samples through 0.45 u Millipore filters. An American Optical temperature compensated refractometer was used to measure salinities. Measurements in the Bellefield creek were obtained on a number of rainless days in June, 1973 and also on June 28, 1973 when a short rain squall occurred at low tide. Measurements in the Charleston Creek were made in June, 1974. The light rain occurred during low tide on June 26, 1974.

RESULTS AND DISCUSSION

Runoff and Erosion

The results of this study are shown in Figure 1. The average pattern of discharge, suspended sediment, and sediment export rate for rainless days is indicated by the broad dashed lines on Figure 1 whereas the results for the stormy day are shown by the solid curves.

In the Bellefield creek the stormy day included two intervals of rainfall. The first began at about low water (hour 1.75) and lasted about seven minutes; about 12 minutes later a second interval of rain began and lasted for five minutes. These intervals are represented by the horizontal bars on the curves on Figure 1. A rain gage located about 50 meters from the weir registered a total of 0.33cm of rain for the two intervals. Thus, the total volume of rain that fell on the drainage basin ($1.7 \times 10^4 m^2$) is approximately 5.6×10^4 liters.

Point A on the storm discharge curve indicates the onset of storm runoff. Point B corresponds to the time when the weir was flooded by the rising tide and all measurements were terminated. The total runoff during this period amounts to about 3.1×10^4 liters. If no rain had fallen, the runoff for this period would have been about 2.3×10^3 liters. If the storm discharge curve is extrapolated from Points B to C by means of the Langbein (1940) procedure, an additional 6.4×10^3 liters of runoff is obtained. Thus the actual volume of rain received by the basin is probably between 3.5×10^4 liters and 5.6×10^4 liters. The discrepancy in the two estimates is probably due to errors in the rain gage, differences in rainfall over the drainage basin area, and in the extrapolation. Infiltration and entrapment of the rain by vegetation may also be minor factors contributing to the discrepancy.

Storm runoff in the Bellefield creek shows three peaks, labeled 1, 2, and 3 on Figure 1. Peak 1 (1.95 l/sec) occurs approximately eight minutes after the onset of rain and nearly coincides with the first suspended sediment peak. The first discharge peak is the result of surface runoff down the bare channel banks which quickly carries large amounts of reddish brown suspended sediment out the mouth of the creek. The second peak in discharge (10.0 l/sec) occurs 22 minutes after the beginning of the first interval of rain and just prior to the onset of the second interval of rain. This peak and its associated lag time are the result of rain accumulation on the flat vegetated surface of the marsh, its subsequent convergence into the channels and passage through the mouth. This component of storm runoff has less erosive power than channel bank runoff because of the gentle gradient of the marsh surface and protection of the marsh surface from raindrop impact by vegetation and numerous small puddles. Entry of this water into the channel causes a dramatic lowering of the suspended sediment concentration. Despite this lowering of turbidity, the sediment export rate maintains a high level compared with that of rainless days,

suggesting that, although suspended sediment peaks are caused by channel bank runoff, major quantities of sediment may also be removed from the flat marsh surface. With the onset of the second interval of rain, a second suspended sediment peak is produced by renewed channel bank erosion. Somewhat later, a third discharge peak (12.5 l/sec), resulting from a new episode of marsh flat runoff, is recorded. The almost exact coincidence of the lag times for peaks 2 and 3 suggest that only rainfall intensity and duration and basin geometry control the runoff process.

The pattern of salinity variation during the storm correlates to a close degree with the discharge and suspended sediment curves. Prior to the storm, salinity maintains a more or less stable value as on rainless days. As can be seen on Figure 1, salinity minima in the Bellefield creek are clearly associated with the first and second discharge peaks. The third discharge peak, however is only associated with a salinity plateau. The rise in salinity after each minima is probably the result of gradual mixing of fresh rain water with saline water on the marsh surface. Water on the marsh surface may be initially density stratified so that somewhat fresher water runs off until convection and diffusion have produced mixing.

A low-tide storm of 0.1cm and ten minute duration occurred on June 26, 1974 in the Charleston Harbor tidal creek. The volume of rain that fell on the drainage basin area of $2.8 \times 10^4 m^2$ is approximately 2.8×10^4 liters. Figure 1 indicates that total runoff between points A and B, i.e. the beginning of the rain flooding of the weir, was 3.6×10^4 liters. Normal runoff for this period is approximately 1.35×10^4 liters, which gives a storm runoff value equal to 2.25×10^4 liters. This value is also less than the actual volume of rainfall indicating that part of the total rainfall was retained in the marsh as observed in the Bellefield creek.

The distribution and order of turbidity and discharge peaks, and salinity minima in the Charleston creek were generally the same as those observed in the Bellefield creek, i.e. turbidity peak, followed by discharge peak, followed by salinity low. However, the discharge peak that accompanied the suspended sediment peak due to channel bank runoff in the Bellefield creek (Figure 1) was not discernible in the Charleston creek. This may be expected since the peak was barely discernible in the Bellefield creek where the rain was nearly 3 times greater than the measured rainfall in the Charleston drainage basin.

Figure 1. Discharge, suspended sediment, salinity, and sediment export rate patterns observed in two small tidal creeks during low-tide storms and low-tide rainless periods. Dashed lines are based on the averages of values observed on rainless days during low slack water and solid curves show the results for the stormy days. Horizontal bars indicate rain intervals.

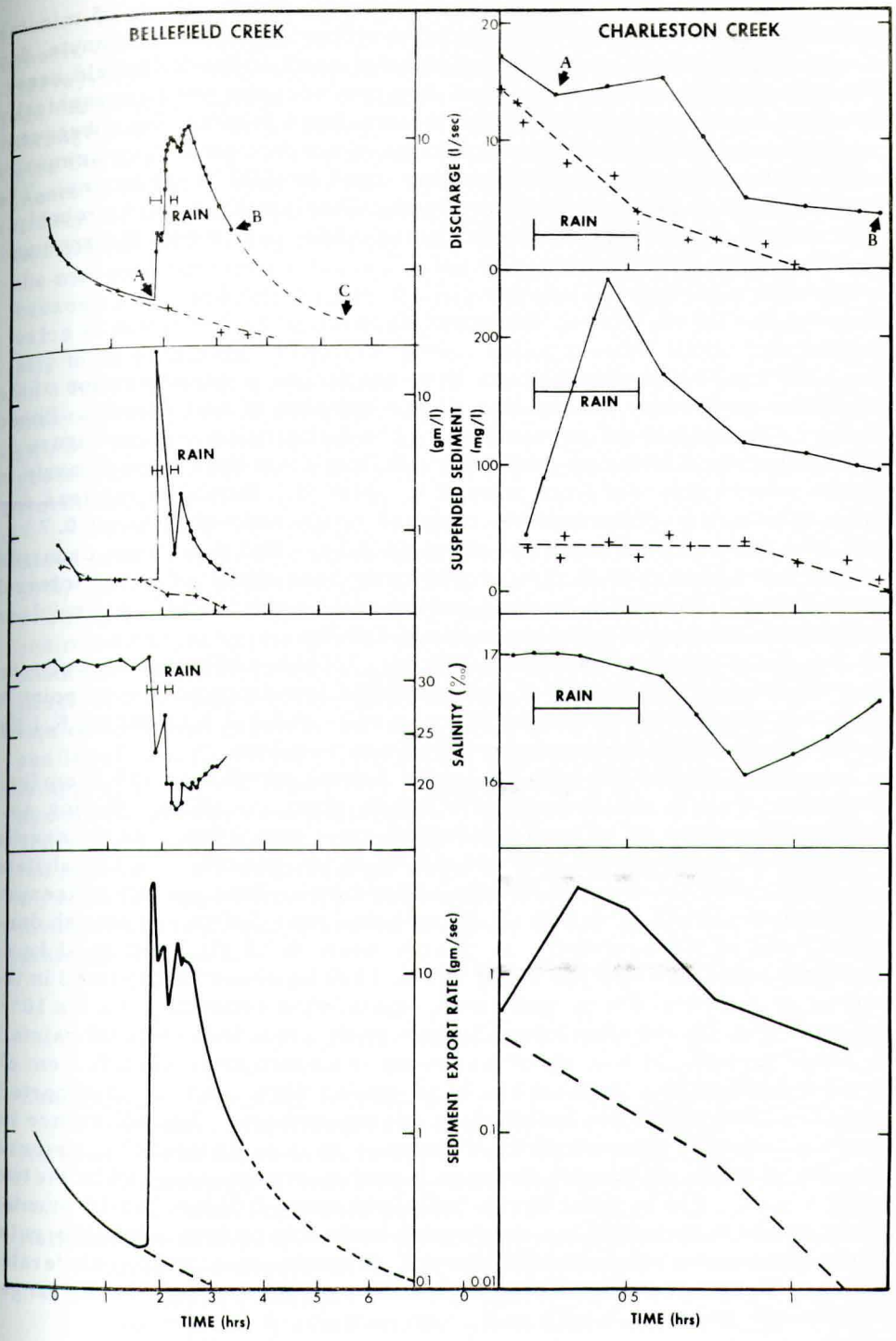
BELLEFIELD CREEK
CHARLESTON CREEK
DISCHARGE (l/sec)
SUSPENDED SEDIMENT (gm/l)
(mg/l)
SALINITY (‰)
SEDIMENT EXPORT RATE (gm/sec)
RAIN
A
B
C
TIME (hrs)
TIME (hrs)

The discharge peak in the Charleston creek occurs 25 minutes after the initial rainfall. This lag time is similar to the 22 minute lag time associated with the second discharge peak in the Bellefield creek. The general agreement of the two lag times in the two geographically removed basins suggests that the accumulated rain and its subsequent convergence in the channels and passage through the mouth is primarily controlled by similar basin geometry found in tidal creek basins. The slightly greater lag time observed in the Charleston creek is probably a combination of greater drainage basin area and runoff distance and smaller rainfall volume.

Sediment Export

We turn our attention in this section to a consideration of the possible significance of low-tide storm erosion in marshlands. Based on the sediment export rate curve for the Bellefield creek on Figure 1, approximately 41.9 kg of sediment was lost from the drainage basin in the 84-minute interval from point A to point B. During a rainless day the sediment export during this interval would amount to about 0.7 kg, thus giving an excess export of about 41.2 kg. Had this storm occurred earlier, an additional 2.3 kg could have been exported in the interval from B to C. During a normal period of low-tide runoff on a rainless day, sediment export amounts to about 4.0 kg.

In the Charleston creek, Figure 1, the sediment export rate curve indicates that 5.6 kg of sediment was lost from point A to point B. Normal release of sediment in this period is about 0.5 kg giving 5.1 kg of sediment export due to storm runoff and erosion.

In the Bellefield area the mean annual rainfall is 119.7 cm/yr. (National Oceanic and Atmospheric Administration, 1973). During approximately one-half of each tidal cycle, the channel banks of the creeks are exposed and vulnerable to erosion by storm runoff. The marsh flats are vulnerable about three-fourths of the time. Thus we can conservatively estimate that about 59 cm of rain per year fall on the marsh during periods of vulnerability. If during each 0.33 cm of rain 41 kg of sediment are lost from the study basin, 7300 kg would be exported in the course of a year. On a unit area basis, this amounts to 4.3×10^{-2} $gm/cm^2/yr$. In the Charleston Harbor study area, mean annual rainfall is 123.7 cm/yr. If 5.1 kg of sediment is eroded from each 0.1 cm of rain, 3,150 kg/yr., or 1.13×10^{-2} $gm/cm^2/yr.$, would be exported from the tidal creek due to low-tide storm erosion. The difference in the two values is a result of the difference in rainfall intensity, or more specifically, the abrasive effects of raindrop impact observed in the two study areas. The rainfall in the Bellefield area, 0.33cm, for 12 minutes, could be characterized as a rain squall or thunderstorm while the rain in the Charleston area, 0.1cm for 10 minutes, was only a moderate storm. Thus our sediment export values represent a significant range of rain-fall intensity.

A study of the weather records (National Oceanic and Atmospheric Administration, 1973, 1974) and the tide tables (National Ocean Survey, 1973, 1974) indicates that mean rainfall intensity in the Charleston creek area during low slack water storms from August 1973, through July, 1974 was 0.22cm/hr. However, the weather records only give the total rainfall for a given hour and do not show smaller increments of rainfall duration and intensity. Assuming, however, that the 0.22cm of rain was continuous during each hour gives 0.036cm of rainfall during each 10 minute interval. This is less than 0.1cm/10min., the measured rainfall intensity in the Charleston creek area. However, because many rainfall events do not fill entire hour long intervals the value of 0.036 cm/10 min. is probably the lowest mean rainfall intensity to be expected. Thus the actual mean rainfall intensity could be 2 or 3 times greater, i.e. close to 0.1cm/10min. The weather record analysis thus indicates that the sediment export rate of 1.13×10^{-2} $gm/cm^2/yr.$, calculated from a rainfall intensity of 0.1 cm/10 min. is probably the better estimate of sediment export resulting from low-tide storm erosion.

The sediment export values of this study, which we feel are based on frequent and representative rainfall events, should be confirmed by additional studies of the effects of high energy events on marshes. The magnitude of our estimates suggests that salt marsh suspended sediment budget studies, and possibly those of estuarine sedimentation, should be designed to include the effects of low-tide storm erosion. To illustrate this point it can easily be shown that the net yearly accumulation of sediment required for vertical marsh growth to keep pace with sea level rise (0.15cm/yr-Shepard, 1964; Stuiver and Daddario, 1963) is approximateyl $0.13 gm/cm^2$ assuming marsh sediment with an average solids density of $0.90 gm/cm^3$. Low tide storm erosion thus represents a negative budget component with a value equal to approximately ten percent of the required net import. Finally as a tentative hypothesis we wish to suggest that low-tide storm erosion may be the chief process involved in the creation and maintenance of low order channels in marsh drainage systems.

REFERENCES

Langbein, W. B., 1940, Some channel storage and unit hydrography studies: Am. Geophys. Union Trans., v. 21, p. 620-627.

National Oceanic and Atmospheric Administration, 1973-1974, Local climatological data (for Charleston, South Carolina): U. S. Dept. of Commerce, Asheville, N. C.

National Ocean Survey, 1973-1974, Tide tables (for Charleston Harbor, South Carolina): U. S. Dept. of Commerce, Rockville, Md.

Powell, R. W., 1951, An elementary text in hydraulics and fluid mechanics: Macmillan Co., New York.

Shepard, F. P., 1964, Sea level changes in the past 6,000 years-possible archeological significance: Science, v. 143, p. 574-576.
Stuiver, M. and Daddario, J. J., 1963, Submergence of the New Jersey Coast: Science, v. 142, p. 951.

ON THE ORIGIN AND HISTORY OF MOUNTAIN LAKE, VIRGINIA

By

Bruce C. Parker
H. Edward Wolfe
R. Vincent Howard
Virginia Polytechnic Institute and
State University
Blacksburg, Virginia 24061

ABSTRACT

This paper compares our findings on the geology of the region near Mountain Lake, Giles County, Virginia with those of previous workers in an attempt to resolve the controversy among previous reports on the lake's origin. The types and estimated positions of formational contacts, calculations of formational thicknesses underlying the lake, and extensive colluvium at the north end support our conclusion that Mountain Lake's origin was by damming of the headwaters of a stream, not by solution or other origins suggested. The extreme fluctuations in the lake level, borne out both by microfossil assemblages and observations in recorded history are explainable by an incomplete damming to the present.

INTRODUCTION

The origin and history of Mountain Lake has attracted interest periodically since its discovery by Gist in the spring of 1751 (Gist, 1751). Such ideas for the lake's origin as that of a volcanic crater and lava flow (Anon. (J), 1897, cited by Ellison, 1948), a glacial cirque or a meteoric crater (cited by Dietrich, 1957) have been ruled out apparently quite effectively by recent investigators. However, the possibilities of damming by talus or slide rock (Rogers, 1884; Sharp, 1933; Hutchinson and Pickford, 1932; and Eckroade, 1962), a solution sink (implied by Nicklin, 1837 and Anon. (J) cited by Holden, 1938; Platt and Shoup, 1950; and Marland, 1967), or a combination of these two types or origin (Dietrich, 1957) have not been adequately supported or laid to rest in our opinion on the basis of information published previously.

While the geology of the Mountain Lake region is vital to an understanding of its origin, the mysterious and dramatic fluctuations in lake level throughout recorded history also have played important roles in formulating and supporting one or more hypotheses concerning the lake's origin. The objective of our study was to review and re-evaluate

data on both the bedrock and geology of the lake basin and on the relevant recorded history of the lake in order to determine the origin of this, the only natural lake in the unglaciated southern Appalachians.[1]

Acknowledgments

We are grateful to The University of Virginia's Biological Station for access to many unpublished notes and papers, to John Byrne (Virginia Polytechnic Institute and State University) and the Forest Products Laboratory (Madison, Wisconsin) for identifying the wood samples, to Charles E. Sears (Virginia Polytechnic Institute and State University) for the grinding of geological samples, to George Simmons (Virginia Polytechnic Institute and State University) and John Slocomb for retrieving submerged tree samples, to Roger Witmer and Ben Johnson (Virginia Polytechnic Institute and State University) for infrared and aerial photography, to Fred May and Marc Sverdlove for geological assistance, to Larry Lane, Hal Sugg, Jim Craft, and Jeff Whitehurst for physical measurements and biological assistance, and to the Gal-Tex Hotel Corporation for permission to conduct this research.

TOPOGRAPHY

Mountain Lake, in Giles County, Virginia, is in the Valley and Ridge Province of the folded Central Appalachians (Figure 5). The highest peak within this area is Bald Knob, at an elevation of 4363 ft (1330 m). Bald Knob forms a part of the crest of Salt Pond Mountain which bounds Mountain Lake to the east. Salt Pond Mountain joins with Johns Creek Mountain, the next structure to the east, to form the southwest end of a major northeast plunging syncline. Ridge crests in the area produce a fairly smooth skyline, with the elevations ranging from 4363 ft (1330 m) to less than 2500 ft (762 m).

Six miles (9.65 km) southwest of Mountain Lake is New River at an elevation of 1600 ft (488 m) which gives a maximum relief in the area of slightly less than 2800 ft (854 m). The greatest local relief occurs nearest the ridges where the elevation may drop as much as 1500 ft (457 m) within 0.5 mi (0.8 km) of the crest.

Mountain Lake occurs at an elevation of 3875 ft (1181 m) and is drained solely by Salt Pond Drain which follows a north-northwesternly course until it joins Little Stony Creek, a tributary of New River.

[1] We do not, however, discount the numerous ponds, mostly less than 1 km^2 surface area, which occur in the Ridge and Valley Province of the Appalachian Mountains (e.g., Watts, 1970).

METHODS

Initially a review of all published and unpublished works on the Mountain Lake area was conducted at Virginia Polytechnic Institute and State University library, The University of Virginia library (notably the Ivy Lewis papers), and records at The University of Virginia Mountain Lake Biological Station to identify all information relevant to the Lake's origin and history. Then, utilizing aerial photographs and geological information largely from Eckroade (1962), we examined the surficial geology in and around the Mountain Lake Basin. Major attention was paid to locating formational contacts, measuring strikes and dips, and comparing aerial photographs including those taken at various seasons with infrared film. Rock and soil samples were collected for examination at Virginia Polytechnic Institute and State University including carbonate content. Measurements of the lake morphometry were conducted for comparison with others. Finally, the species of trees and shrubs in the watershed were recorded, and specimens of several submerged, in place tree trunks were collected from the lake by SCUBA diving for identification and dating by the radiocarbon method.

GEOLOGY

Structurally, Mountain Lake is on the crest of an anticline that plunges northeast at about 7.5°; limbs dip approximately 10°. Plunge values as low as 5° (Holden, 1938) and as high as 10° were noted. The underlying geological structure of Mountain Lake (Figure 1) and our geological profiles (Figure 2) reflect these averaged observed values; the three structural sections in Figure 2 depict formational occurrence with depth for lines A-A', B-B', and C-C' indicated in Figure 1. These conclusions generally agree with those of Sharp (1933), Holden (1938), and Eckroade (1962), whose studies constitute much of the previous available information on the geology of the lake basin.

Precise location of the formational contacts shown in Figures 1 and 2 was possible only on the western side of the lake basin. The Martinsburg Shale --- Juniata Sandstone contact was readily apparent along Virginia Route 700 which parallels the west side of the lake. This shale possesses numerous brachiopod fossils of the species Orthorhynchula stevensoni and Lingula nicklesi, which characterize the Maysville, the uppermost division of the Martinsburg (Rader and Ryan, 1965). Soils and vegetation also signaled the Martinsburg Shale --- Juniata Sandstone contact. A characteristic light yellow loam with considerable clay and a pH range of 7.2-7.5 overlay the Martinsburg Shale, while sandy soil often somewhat pink with a pH range of 5.6-5.9 overlay the Juniata Sandstone. The area underlain by Martinsburg Shale contains a beech (Fagus grandiflora Ehrh.)--northern red oak (Quercus rubra L.) forest, at least part of which apparently comprises a climax

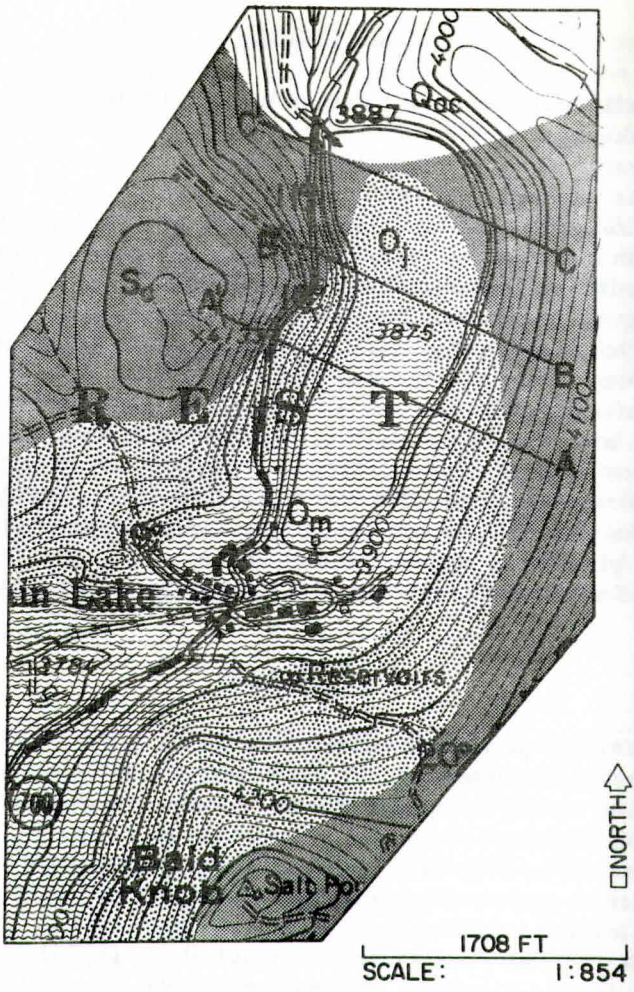

Figure 1. Underlying geological structure of Mountain Lake showing apparent contacts between Ordovician Martinsburg (Om), Ordovician Juniata (Oj), Silurian Clinch (Sc), and Quaternary Alluvium-Colluvium (Qac); position of profile views of underlying geology, A-A', B-B', and C-C'; and location of strike and dip calculations for 10°, 11°, 19° and 20° (by H. E. Wolfe).

stand. Contrastingly, a virgin hemlock (Tsuga canadensis (L) Carr.) --- rhododendron (Rhododendron maximum L.) climax forest assumes dominance on the area underlain by the Juniata Sandstone and the Tuscarora Sandstone. The residual soil derived from the Tuscarora Sandstone is yellow and sandy generally with a pH range of 4.5-5.2. Our

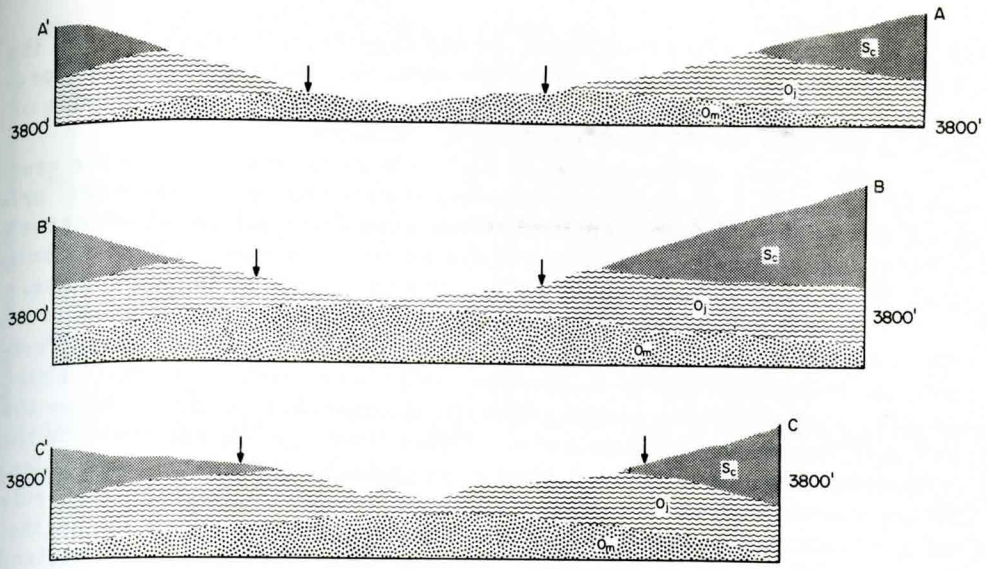

Figure 2. Profiles of underlying geological formations of Mountain Lake area corresponding to (surface) overhead locations on Figure 1: A-A', B-B', and C-C'; arrows indicate perimeter of lake basin and the elevation of 3800 ft is a reference point in each profile; geological structures are Ordovician Martinsburg (Om), Ordovician Juniata (Oj), and Silurian Clinch (Sc). Scale 1:100 (by H. E. Wolfe).

calculations based on measurements made along Virginia Route 700 indicate an approximate thickness of 145 ft (44 m) for the Juniata, which is intermediate between 130 ft (40 m) claimed by Holden (1938) for the same location and the minimum thickness of 190 ft (58 m) cited by Eckroade (1962) for the formation in general. From our data, the contact of the Juniata and Tuscarora Sandstones follows a northeasterly direction toward the lake's edge but appears to turn northward, as shown in Figure 1, such that only the northernmost end of Mountain Lake probably is underlain by Tuscarora Sandstone.

The northern rim of Mountain Lake basin adjacent to the shoreline is characterized by blocks of Tuscarora intermixed with smaller purple sandstone blocks derived from the Rose Hill Formation which overlies the Tuscarora and occurs in place on the higher ridges at the north end of the basin. The orientation of the bedding planes in the blocks of Tuscarora and the frequent occurrence of blocks of Rose Hill beneath those of Tuscarora at the northern end of Mountain Lake indicate an area of colluvium or talus (slide rock). As shown in Figure 1, this colluvium, derived primarily from the Tuscarora and, to a lesser degree, the Rose Hill Formation, continues around much of the eastern shoreline of the lake. Contacts east of the lake were not located because

of colluvium, but aerial photographs and the general distributions of the hemlock-rhododendron and beech-oak communities suggested the approximate positions of contact shown in Figure 1 and this agrees, more or less, with Eckroade's (1962) estimated contacts.

We found neither igneous nor metamorphic rock in the area which would have indicated the possibility of volcanic or meteoritic origin. Nor did we observe any indication of past glaciation, which agrees with Fiedler (1967) who placed the southernmost extension of past glaciation in the Appalachians about 78 mi (125 km) north of Mountain Lake.

No carbonate-rich Martinsburg shale was found in the lake basin. The nearest shale with a carbonate content of 50 percent was found outside the watershed and at a stratigraphic level within the Martinsburg which, by calculation, would place it at least 200 ft (61 m) below the present bottom of Mountain Lake. These findings do not preclude the possibility of carbonate-rich Martinsburg Shale in the lake basin before the origin of the lake, as suggested by Holden (1938), nor can one rule out the presence of carbonate-rich shale beneath the colluvium on the eastern shore of the lake. However, the microfossils data of Marland (1967) from sediment cores of Mountain Lake give no support for carbonate-rich water during any period in the lake's sediment history.

FLUCTUATIONS IN WATER LEVELS OF MOUNTAIN LAKE

Figure 3 summarizes reports of the lake's water level since its discovery. Especially noteworthy were the two (possibly three) periods when Mountain Lake went nearly dry, namely 1768-1804 and 1865-1869, (Platt and Shoup, 1950; Lewis, 1957). Historical accounts of these low-water episodes indicate that water remained in the deepest depression of Mountain Lake (Figure 4). Scientific data supporting one or more previous period of low-water level in the lake include rooted submerged stumps of trees observed by various persons and Marland's (1967) studies of various sediment cores from Mountain Lake revealing at least two microfossil assemblage zones when littoral cladoceran species dominated over planktonic ones. Based on an estimated 1.0 mm/yr sedimentation rate, Marland calculated that the most recent episode of dominant littoral cladocerans was that of the 1768-1804 period.

Three rooted tree trunks from depths of 20-30 ft (6.2-9.3 m) below maximum water level at the northwestern end were collected. Tree trunks were not found in place below 30 ft, a depth which would make the shoreline of the lake circumscribe about one half its present area (Figure 4). Two of the tree specimens were identified as hemlock and one as a southern yellow pine; identifications were confirmed by the U. S. Forest Products Laboratory, Madison, Wisconsin. On the basis of known climate at Mountain Lake, tree species presently in the area, and knowledge of forest tree environmental tolerances (Fowells, 1965), the southern yellow pine most likely is a pitch pine (Pinus rigida

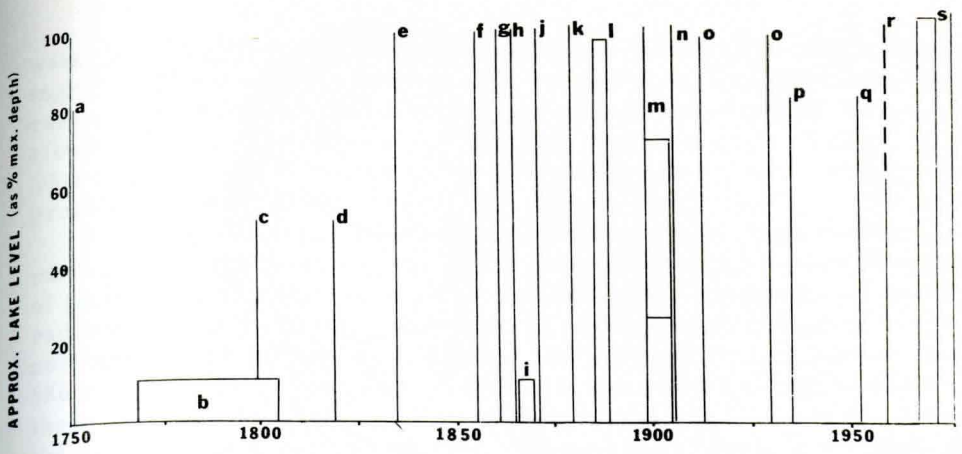

Figure 3. Approximate chronology of observed water levels in Mountain Lake interpreted from historical records*. X axis = year of observed lake level; Y axis = estimated maximum depth of lake in feet or as percent of maximum possible depth (i. e., 100 ft = 100% full).

*Sources of lake level observations or records shown in Figure 3:

A Description by Gist (1751) (IN: Darlington, 1893), who discovered the lake (Pownall, 1776; Summers, 1923; Mulkearn, 1954)

B Small pond at north end 1768-1804 (Johnson, 1906); still low in 1804 (Roberts, cited by Lewis, 1957)

C 1794 deed to property showing sketch of lake (Marland, 1957)

D Half full by 1820 (Lewis, 1957)

E Full by 1835 (Rogers, 1884)

F Full by 1855 (painting by Robert Beyer; see Wright, 1973)

G Full in 1861 (Pollard, 1871; Pendleton, 1920)

H Full in 1864, according to Major Barrett (Lewis, 1957)

I Single small pond at north end with trees in place in lake basin, ca. 1865-69, according to Mrs. Ingles (Lewis, 1957)

J Full in 1871 (Pollard, 1871; Pendleton, 1920)

K Full in 1879 (Chapman, 1949)

L Slightly below full, 1885-88, according to Mrs. Ingles (Chapman, 1949; Lewis, 1957)

M About 20-30 ft below full level 1898-1904 (Chapman, 1949); however, full according to Campbell (1898)

N Full in 1904-5 (Dietrich, 1957)

O Reasonably full in 1913 and 1930 (Chapman, 1949)

P 1935, a moderate drop in lake level (Lewis, 1957)

Q 1952-53 aerial photograph, U. S. Department of Agriculture - Soil Conservation Service

R 1959 spring, relatively low level until earthquake, then rapid filling (Mrs. Robert Dollinger, Pers. Comm. 1973)

S Observations of B. Parker, 1969 to present

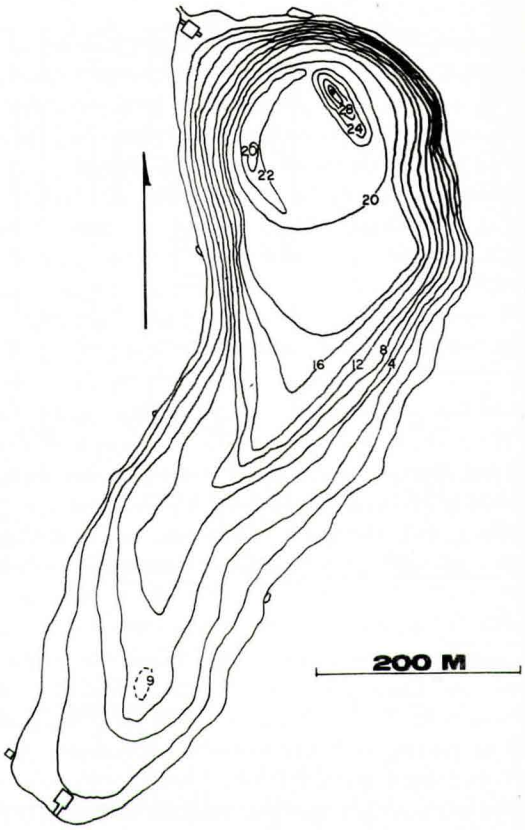

Figure 4. Morphometric map of Mountain Lake modified from Deevey, Jones, and Daly (1957), as cited by Marland (17); dotted contour line display approximate area of depths not reported by previous studies.

Mill.) or table mountain pine (Pinus pungens Lamb.). Of interest also is the report by Lewis (1957) of a "white pine" (presumably Pinus strobus L.) with approximately 200 annual growth rings collected from shallow water at the northwest margin of the lake. Pine species commonly invade open fields and are generally intolerant of shale and water-saturated soils (Fowells, 1965). Furthermore, the southern yellow pine specimen possessed at least 30 annual growth rings and was in an excellent state of preservation. Radiocarbon dating of wood from the outer cortex of this specimen by Teledyne Isotopes, New Jersey, revealed an age of 295 $\pm$ 80 years B. P. This yellow pine, therefore, apparently sprouted and grew at the periphery of Mountain Lake in approximately 1655 $\pm$ 80 A. D., which preceded the 1768-1804 period of low

water level found in the earliest historical records (Figure 3). Interestingly, Marland's (1967) 1.0 mm/yr estimated average sedimentation rate and microfaunal data also suggest an earlier period of low water in Mountain Lake approximately 1656-1726, with a peak low level at 1691. This period is a reasonable match for our radiocarbon date on the outer growth rings of the yellow pine.

Closer examination of Marland's sediment core lengths and radiocarbon dates, however, suggests the possibility of even earlier periods of prolonged low water level in Mountain Lake. Marland reported two radiocarbon dates on organic matter in sediment cores from the deeper northern end of the lake (i.e., 910 $\pm$ 110 years B.P. for a core depth of 620 mm and 1760 $\pm$ 120 years B.P. for a core depth of 740 mm). From these, we calculate mean sedimentation rates of 0.68 and 0.42 mm/yr; the average would be 0.55 mm/yr. If one applies these calculated sedimentation rates, rather than the 1.0 mm/yr value apparently arbitrarily chosen by Marland, the two periods of dominant littoral/planktonic cladocerans become 1561 or 1701 (average 1639) and 1311 or 1538 (average 1466). The radiocarbon date on the outer growth rings of the southern yellow pine (i.e., 1655 $\pm$ 80) would on this basis, more likely apply to the more recent calculated low water level, which nevertheless would be earlier than the reports in the historical record (i.e., 1768-1804). Furthermore, if sedimentation rates as low as 0.68-0.42 mm/yr, instead of 1.0 mm/yr, occurred, then Marland might have missed the zone of approximately 15 mm at higher levels in his sediment cores which represented the 1768-1804 period of low water level in recorded history.

We have made rough approximations of the annual precipitation, estimated evapotranspiration and runoff in Pond Drain. Less than half of the water entering the basin apparently leaves by a combination of runoff through Pond Drain and evapotranspiration. Moreover, during dry periods seasonally, the lake level drops at a rate which can only be accounted for by underground seepage or other loss. During these dry periods, while Pond Drain has no obvious water in it, one can hear water flowing at some depth below ground level, suggesting an underground stream below the colluvium.

CONCLUSIONS

Based on the geology of the Mountain Lake basin, we conclude that the origin of Mountain Lake is from damming by talus (slide rock) as proposed earlier (Rogers, 1884; Hutchinson and Pickford, 1932; Sharp; 1933; and Eckroade, 1962). Thus the origin of Mountain Lake corresponds to Type 20a of Hutchinson's (1957) classification.

Hutchinson also cites Mountain Lake as an example of Type 20a origin. Although he presents no further details on Mountain Lake, Hutchinson notes, "When the stream is small and the landslide large, a

permanent dam may be produced . . . ," and "Sufficiently large slides are most apt to occur in mountain valleys in which a stream is eroding a relatively soft rock overlaid by more resistant material which thus may be undercut." The Juniata has considerably less cementing substances than the overlying Tuscarora and Rose Hill Sandstones, which meets the requirements for extensive undercutting.

The depression now occupied by Mountain Lake apparently resulted from the breaching of an open, northeast-plunging anticline. Erosion by Salt Pond Drain, which flows gradually north, has been slow because the resistant sandstones, which overlie the relatively easily eroded Martinsburg Shale exist in place at the south end of the lake and near the head of Doe Creek. A much more impressive valley than that formed by Salt Pond Drain has been developed by Doe Creek which failed by very little to reach and drain Mountain Lake by head water erosion; however, Doe Creek may be related to an older New River erosional surface. Thus, originally a stream valley developed on the axis of the anticline. Salt Pond Drain may have followed a course somewhat eastward of its present location as suggested by the contours on a topographic map (Figure 5). Marland (1967) pointed out that the first deed of ownership of the area in 1789, shows a sketch of the lake, then called Salt Pond, which appears about half as large as the present surface area, and apparently had an overflow seemingly eastward of the present Pond Drain.

Today large Tuscarora blocks form a colluvial dam where Salt Pond Drain leaves the lake basin. Damming may have been gradual or sudden. While the ice sheets to the north were retreating, snow and ice would continue to cover mountains in the area. During this postglacial period, as Fiedler (1967) noted, freeze-thaw cycles would be common in the Mountain Lake area, and large blocks of Tuscarora may have begun the damming process following the close of the Pleistocene Epoch (i. e., ca. 7,000-9,000 yrs ago). However, earlier glacial action cannot be ruled out. We note that Marland (1967) obtained a maximum age of 9,180 $\pm$ 330 years for his deepest sediment core sample from Mountain Lake, but for unstated reasons, he concluded that the lake formed about 2,000 years ago.

The possibility that one or more catastrophic events may have caused the damming also cannot be ruled out. Bollinger's (1) records of earthquakes in recent times reveals that the area is one of considerable activity.

Periodic fluctuations in the lake's level were cited by Holden (1938) as major supporting evidence for the solution origin of the lake basin. However, the shape of Mountain Lake and the geology of the basin are not compatible with sinkholes. Cooper (1964) and Fiedler (1967) found no sinkholes in Martinsburg shale, even in the lower carbonate-rich layers. Second, even if solution had occurred, Cooper (1964), in reference to the Walker Mountain tunnel through a complete section of Martinsburg, stated that the remaining insoluble residue was

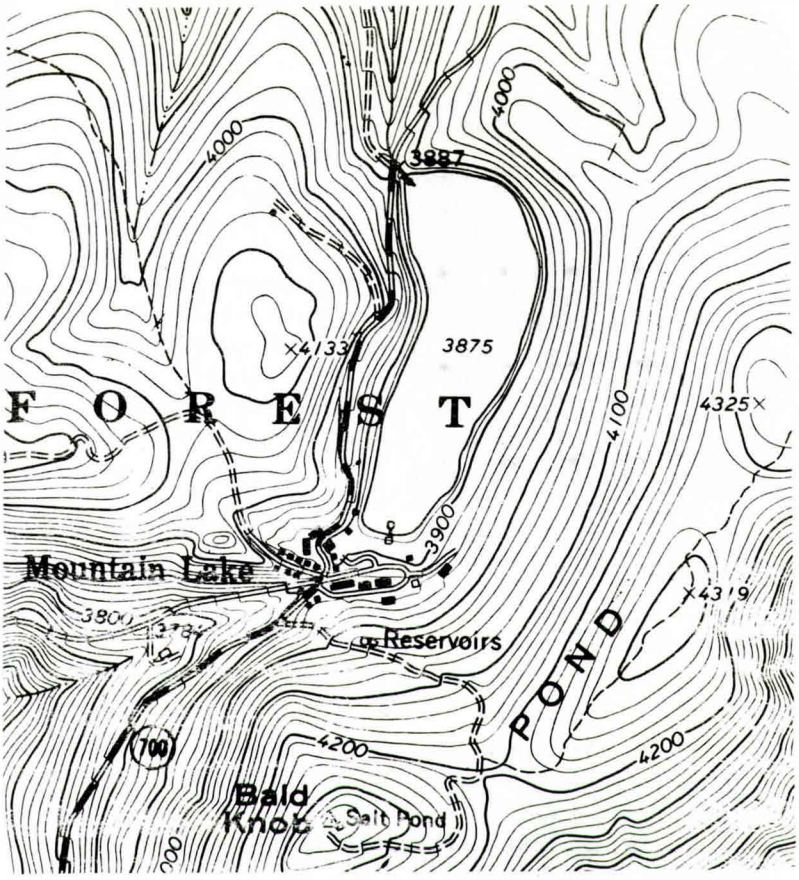

Figure 5. Portion of state of Virginia topographic map of Mountain Lake area.

adequate to prevent collapse. A true sinkhole in the upper Martinsburg would have to extend upward through at least 50 ft (15 m) of Juniata to reach the bottom of Mountain Lake, then further dissolve through 1500 ft (457 m) of Martinsburg to make a sinkhole. Also, if a sinkhole, the lake should have totally drained when unpuddled (i. e., temporarily unstopped or unoccluded). As previously noted, historical accounts of the dropping of the lake level indicate that water remained in one or more locations at the north end of the lake basin and that the basin never went totally dry (Figure 3). Therefore, we suggest that the two or more deep spots at the north end of the lake represent depressions not entirely filled by the damming processes (Figure 4). The rapid seasonal fluctuations in the lake level can be accounted for entirely on the basis of incomplete damming of the original stream valley. Thus, the apparent numerous periods of low water level in Mountain Lake since its origin, at least some of which in recent times have accompanied invasions of the open shoreline area by pines and other forest species, might

well have been caused by drought and/or change in dam permeability.

Additional evidence for the origin of Mountain Lake could be obtained by core drilling, an activity not presently permitted in the basin. Were such possible, the area at the north end of the lake near the location of the presumed dam and adjacent to Pond Drain should be ideal. Drilling in this area might recover samples of the bedrock. Additional radiocarbon dates from sediments and submerged tree trunks, along with studies of the pollen, spores, and/or other microfossils, also might provide data concerning the age and origin of Mountain Lake and more accurately fix the dates of lake fluctuations. For example, if the lake first began to form shortly following the last glaciation to the north, a kind of tundra vegetation with grasses dominating would be expected, and the pollen and spores in the deeper sediments should confirm this point, or possibly show that the basin developed much earlier. Based on our conclusion that Mountain Lake's origin was by damming, it follows that major seismic activity today could alter the level of the lake dramatically.

REFERENCES CITED

Bollinger, G. A., 1969, Seismicity of the central Appalachian states of Virginia, West Virginia, and Maryland - 1758 through 1968: Bull. Seismological Society of America, v. 59, p. 2103-2111.

Campbell, M. R., 1898, Earthquake shocks in Giles County, Virginia: Science (N. S.), v. 7, p. 233-235.

Chapman, H. H., 1949, Yale professor discusses Mountain Lake enigma: Virginia & Virginia County, v. 3, no. 2, p. 27.

Cooper, B. N., 1964, Relation of stratigraphy to structure in the southern Appalachians, In: Lowry, W. D. (ed.), Tectonics of the Southern Appalachians, Virginia Polytechnic Institute, Department of Geological Science Memoir 1, Stone Printing and Manufacturing Company, Roanoke, Virginia, p. 81-114.

Darlington, W. McC., 1893, Christopher Gist's Journals, with historical, geographical, and ethnological notes and biographies of his contemporaries: Arthur H. Clark Company, Cleveland, Ohio.

Dietrich, R. V., 1957, Mountain Lake: Mineral Industries Journal, v. 4, no. 2, p. 7-8.

Eckroade, W. M., 1962, Geology of the Butt Mountain Area, Giles County, Virginia: M. S. Thesis, Department of Geology, Virginia Polytechnic Insitute, 64 p.

Ellison, B., May 30, 1948, Letter to Goodridge Wilson, In The Southwest Corner, Roanoke Times.

Fiedler, F. J., 1967, Surficial geology of the Mountain Lake area, Giles County, Virginia: M. S. Thesis, Department of Geology, Virginia Polytechnic Institute, 111 p.

Fowells, H. A., 1965, Silvics of forest trees of the United States

(Forest Service), United States Department of Agriculture, Agriculture Handbook No. 271. Washington, D. C.: U. S. Government Printing Office, 762 p.

Gist, Christopher, 1751, Journal of Christopher Gist, 1750-51: Edited by J. S. Johnston, Filson Club Publications, no. 13, p. 161.

Holden, R. J., 1938, Geology of Mountain Lake, Virginia: Virginia Academy of Sciences Proceedings, 1937-38, p. 73.

Hutchinson, G. E., 1957, A treatise on limnology: v. 1, John Wiley & Sons, New York, 1015 p.

Hutchinson, G. E. and Pickford, Grace E., 1932, Limnological observations on Mountain Lake, Virginia: Internationale Revue Gesarrten Hydrobiologie, 27, no. 2/3, p. 252-264.

Johnson, D. E., 1906, A History of Middle New River settlements and contiguous territory: By the author, Huntington, West Virginia, 500 p.

Lewis, I. F., 1957, A history of Mountain Lake: unpublished manuscript, Newman Library, Virginia Polytechnic Institute & State University, Blacksburg, 26 p.

Marland, F. C., 1967, The history of Mountain Lake, Giles County, Virginia: An interpretation based on paleolimnology, Ph. D. Thesis, Biology Department, Virginia Polytechnic Institute, 129 p.

Mulkearn, Lois, 1954, George Mercer Papers relating to the Ohio Company of Virginia, compiled and edited by Lois Mulkearn: Darlington Memorial Library, University of Pittsburgh Press, 731 p.

Nicklin, P. H., (Peregrine Prolix, pseud.), 1937, Letters descriptive of the Virginia springs, etc.: H. S. Tanner, Philadelphia, 248 p.

Pendleton, W. C., 1920, History of Tazewell County and southwest Virginia, 1748-1920: W. C. Hill Printing Company, Richmond, Virginia, p. 181-183.

Platt, R. B. and Shoup, C. S., 1950, The use of a thermister in a study of summer temperature conditions of Mountain Lake, Virginia: Ecology, v. 31, no. 3, p. 484-488.

Pollard, E. A., 1871, A trip to New River, Salt Pond, Bald Knob and Little Stoney Creek: The Virginia Tourist, Lippincott, Philadelphia, Pennnsylvania, p. 130-149.

Pownall, T. M., 1776, A topographical description of such parts of North America as are contained in (annexed) map of the middle British Colonies and in North America: Printed for J. Almon, opposite Burlington House, in Piccadilly, London, MDCCLXXVI, 16 p.

Rader, E. K. and Ryan, J. J., 1965, Martinsburg formation in west-central Virginia: Virginia Minerals, v. 11, p. 32-34.

Rogers, W. B., 1884, Report on geological reconnaissance of the state of Virginia, made under the Appointment of the Board of Public Works, 1835, In: Geology of Virginias, D. Appleton Co., New

York, N. Y., p. 109-110.
Sharp, H. S., 1933, The origin of Mountain Lake, Virginia: Journal of Geology, v. 41, no. 6, p. 636-641.
Summers, L. P., 1929, Annals of Southwest Virginia, 1769-1800: By author, Abington, Virginia 921 p.
Watts, W. A., 1970, The full glacial vegetation of northwestern Georgia. Ecology 51: 18-33.
Wright, L., 1973, Edward Beyer and the Album of Virginia: Virginia Cavalcade, v. 22, no. 4, p. 36-47.

DETECTION OF SUBSURFACE SOLUTION CAVITIES IN FLORIDA USING ELECTRICAL RESISTIVITY MEASUREMENTS

By

Douglas L. Smith
and
Anthony F. Randazzo
Department of Geology
University of Florida
Gainesville, Florida 32611

ABSTRACT

Preliminary electrical resistivity investigations in a low-relief karst terrain with a shallow water table provide a simple and inexpensive technique to identify possible water-filled solution cavities at shallow (0-50 feet) depths. Values from profiling and sounding measurements employing the Wenner electrode arrangement in Citrus County, Florida, were interpreted as indicative of solution cavities at a depth of 38 feet at one site and 20 feet at another. A shallow drilling program at the sites encountered solution voids at these depths, substantiating the effectiveness of the method. In addition, the measurements suggest lateral extent of the subsurface cavities and demonstrate a valuable auxiliary tool for the planning of drilling programs to detect subsurface cavities.

INTRODUCTION

The topography of a considerable portion of north-central Florida is influenced by the presence of a thick sequence of carbonate rocks belonging to the Avon Park Formation and Ocala Group of Eocene age. Characteristic karst features, including minimal surface drainage, solution cavities, and sinkholes, are evident in this region. The importance attributed to the detection of near surface (0-50 feet) solution cavities is due in part to problems they pose for the planning of major construction projects, housing developments, and nuclear power plant locations. This report presents the results of a limited test to determine the feasibility of subsurface solution cavity detections with electrical resistivity measurements. Our goal was to correlate resistivity anomalies indicative of solution cavities with known voids detected by a shallow drilling program.

Resistivity methods have traditionally been regarded to be of

limited value for geophysical exploration, having applications only for unique situations. Heiland (1940) and Jakosky (1950) have comprehensively summarized the theory and practical uses of electrical exploration whereas Van Nostrand and Cook (1966) have exhaustively treated the concepts of interpretation of data. Bristow (1966) presented a new technique for the detection of subsurface cavities which involved placing one of four electrodes at a distance of effective infinity. Philips and Standing (1969) discussed a more complicated, but essentially similar, process for the electrical detection of caves. A recent report (Bates, 1973) summarizes all geophysical methods for the detection of subsurface cavities and regards electrical resistivity measurements as most promising. Bates presented results of research designed to test and improve the Bristow Method.

Measurements of electrical resistivity were made during April, 1974, in Citrus County (Figure 1) about 3 miles west of Homosassa Springs, Florida. The area studied represented a portion of a large (one square mile) tract of land that had been cleared of brush and small trees, leveled with a maximum of three feet of fill, and surveyed for commercial development. The general elevation is approximately 8 feet above sea level and the water table was between 3 and 5 feet below the surface at the time of the survey. The Inglis Formation (Puri and Vernon, 1964) is exposed at the surface and, except for the thin overburden of fill and numerous subsurface water-filled cavities, should appear electrically as a homogeneous medium.

The area was first investigated for subsurface cavities by means of 38 drill holes located on a grid pattern having an equal spacing of 300 feet. Two of these holes were cored to a depth of 65 feet. The remaining holes were wash borings to depths of either 25 or 75 feet. Resistivity surveys were conducted about wash boring DH 23 (75 feet deep) in order to verify the detection ability for a large solution cavity known to exist between 38 and 45 feet. This wash boring encountered moderately hard Inglis limestone at a depth of three feet below the drilling surface. Resistances offered to drilling by the subsurface rocks varied with depth and only soft limestone occurred directly below the cavity for six feet. The very hard rock below a depth of 58 feet was probably dolostone.

Wash boring DH 34 (25 feet deep) was selected for a resistivity survey in order to test the detection ability for a shallow cavity which occurred between 15 and 19 feet. Rock encountered in wash boring DH 34 was generally softer than that in DH 23. Drill hole DH 33 was included in this resistivity survey because of its proximity to DH 34 and to document the actual rock types present. The log for drill hole DH 33 is shown in Table 1.

Ground-water solution is usually greatest in a thin zone just below the water table which fluctuates with changes in sea level (Stringfield and LeGrand, 1966). The great extent of sea level changes during the Pleistocene has caused vertical migration of zones of maximum

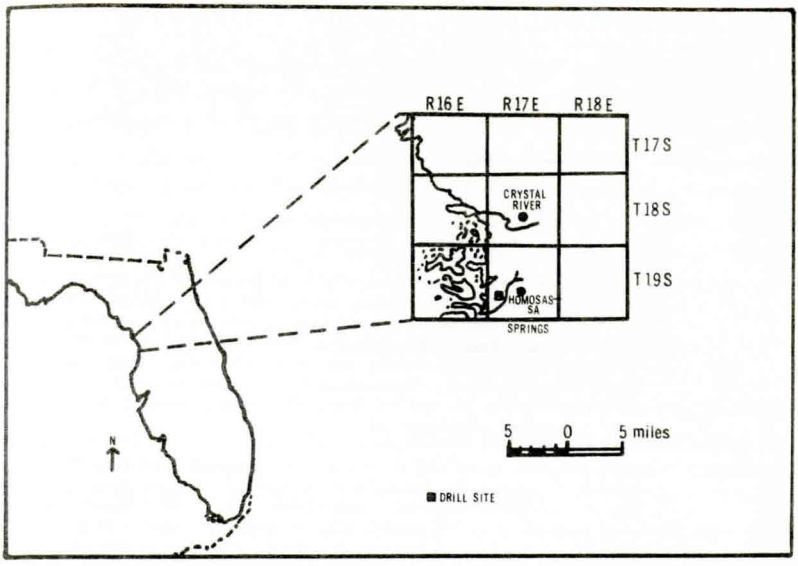

Figure 1. Index map of drill site area.

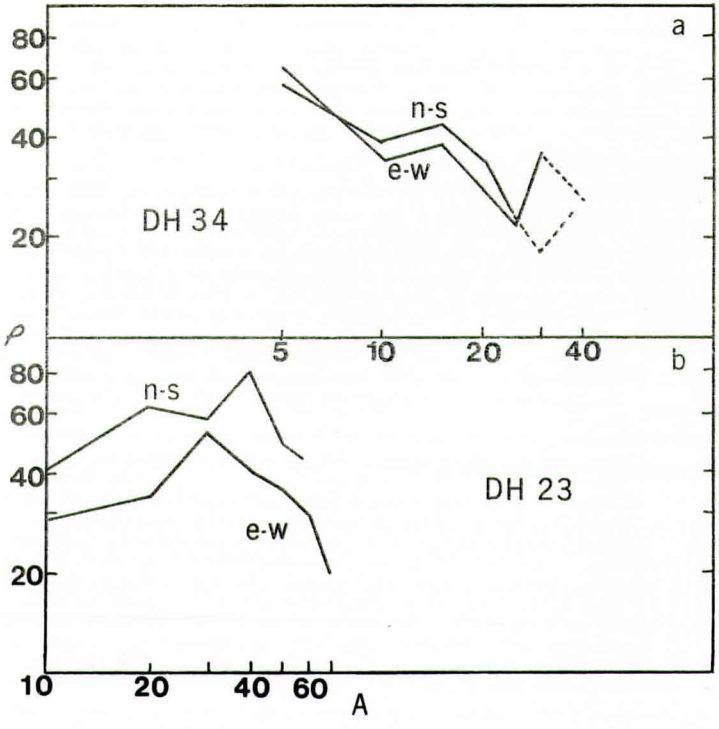

Figure 2. Apparent resistivity (ρ) in ohms-feet versus electrode spacing (A) in feet for drill holes DH 23 and DH 34. Data for both north-south and east-west electrode arrangements are shown.

Table 1. Core Log for Drill Hole 33 Homosassa Springs, Florida (Limestone Classification from Dunham, 1962).

Depth	% Recovery	Description
0-3'	---	Fill
3-8'	99%	Well lithified, creamy white, recrystallized packstone; Most of the grains are fossil fragments of foraminifera, pelecypods, gastropods, bryozoans and echinoid plates (Fibularia). Drusy calcite coats many of the grains. The limestone is moderately porous with moldic, inter-particle and vug types predominating. Approximately one foot of more friable foraminiferal packstone occurs at 5-6'. There is a sharp contact between friable and well lithified packstone at 6'.
8-18'	75%	Well lithified, creamy white, recrystallized packstone with occasional lenses of friable foraminiferal packstone; Faunal assemblage is similar to above. Porosity generally decreases from 10-18'; moldic porosity is the most common type. Cavities encountered at 12-13' and 15-17'.
18-28'	20%	No cavities; poor recovery due to extremely friable nature of the limestone which disaggregates easily when drilled. A few thin but harder layers were inferred from the drilling resistance. Recovered limerock resembles the friable packstone described above; little recrystallized packstone was recovered.
28-38'	80%	Gradual loss of circulation after encountering one foot cavity at 34-35'. White friable packstone quickly passes into more lithified, recrystallized packstone with moldic porosity. This packstone is less porous than those found above. It is abundantly fossiliferous, containing numerous foraminifera, pelecypods (including Blagraveia and Fimbria), and echinoids (Periarchus lyelli common).
38-48'	65%	Circulation lost at 44' but no cavity encountered; very low drilling resistence at 40-43'. Very soft, friable, white packstone grading downward to a gray, poorly consolidated, sandy clay which passes into a well lithified, grayish, slightly dolomitized, finely crystalline packstone with few fossils. This lithology grades downward to a friable, coquina-like grainstone comprised of foraminifera and mollusk fragments, poorly cemented. The grainstone is underlain by a very porous but lithified and slightly dolomitized grayish, medium crystalline packstone which passes to a grayish brown, well lithified dolostone with abundant pelecypod molds. This dolostone first ocurs at 45½' and is underlain by a more finely crystalline yellowish-brown dolostone which is more friable and contains almost no fossils.
48-55'	60%	Hard, finely crystalline brown dolostone becoming more poorly consolidated and clay-rich in places. Drilling resistance varies from very hard layers to very soft zones to hard but fragmented layers. The hard dolostone has low porosity and is only slightly fossiliferous. A zone of poorly consolidated clayey, dolomitic sand occurs at approximately 53'.
55-65'	100%	Hard, brown dolostone with several zones of slightly greater moldic porosity; three zones of disaggregated clayey and sandy dolomite occur at 57', 61', and 63'. Dolostone between 55-63' is moderately laminated and fine grained; between 59-62' it contains abundant intraclasts but few fossils. Moldic porosity increase in the last foot of core (64-65').

solution. Porosity and permeability trends develop along original faunal distributions and are dependent on aragonite, low-Mg calcite, and high-Mg calcite ratios in shells and skeletons. The abundant moldic porosity found in this area suggests such an origin (Textoris et al., 1972). The larger solution cavities encountered may represent an enlargement of moldic pores to the extent of creating nonfabric selective vugs, which eventually merge into a substantial cavity. The role of joint solution could not be documented in this study area.

Acknowledgments

We are grateful to G. Maddox of the Norrin Corporation and to F. M. Wahl for encouragement to undertake this project and to S. Denahan of the Florida Department of Transportation for lending us the appropriate resistivity equipment. G. Taylor and G. Stone provided valuable field assistance. D. Spangler critically reviewed the manuscript and provided helpful suggestions for its improvement. This investigation was partially supported by an Annual Allotment Grant from the Florida Center of the Office of Water Resources Research.

RESISTIVITY MEASUREMENTS

The basic procedure of the resistivity method is to measure at the surface the potential gradient associated with a known current flowing into the earth. Anomalies in electrical conductivity at depth appear as variations of the potential drop. The recorded variable is an apparent resistivity and reflects an averaging effect of electrical resistance through all material penetrated.

All measurements were made with a Keck Earth Resistivity meter model VB-63, which permitted manual control of current flow direction and provided for accurate nulling of self potentials. Due to the reconnaissance nature of the investigation, the Wenner configuration of four equally spaced electrodes was used exclusively. Both sounding and profiling data were collected, with several electrode arrays arranged perpendicularly about bore hole sites.

Table 2 lists sounding data for various east-west and north-south electrode spacing centered on drill holes DH 23 and DH 34. Values recorded during repetitive measurements are also given. In all cases, the value ρ is the product of resistance in ohms and electrode spacing in feet. Figure 2 depicts graphs in the conventional log-log manner (Van Nostrand and Cook, 1966) of apparent resistivity, ρ, versus electrode spacing for sounding measurements about drill holes DH 23 and DH 34.

Profiling measurements, those with a constant electrode spacing but with array centers moved throughout a perpendicularly arranged grid pattern, were made about drill holes DH 23, DH 33, and DH 34.

Table 2. Sounding data for east-west and north-south oriented resistivity measurements over drill holes DH 23 and DH 34. "A" is electrode spacing in feet and ρ is apparent resistivity in ohms-feet. Asterisk (*) indicates low confidence value due to self potential uncertainties.

	DH 23		DH 34	
A	E-W	N-S	E-W	N-S
5			61, 70	58, 58
10	29, 28	36, 46	33, 35	37, 40
15			38, 38	39, 48
20	46*, 34	50, 80	28, 28	32, 36
25			22, 24	22, 25
30	57, 48	54, 64	33, 38	12, 28
40	40, 40	64, 104	26	27
50	36, 36	40*, 50		
60	38*, 30	37, 51		
70	19	56*		

Measurements were made on north-south and east-west axes with the electrode array centered on, but perpendicular to, the axis. Table 3 lists the results. Based on drilling results and sounding data, an electrode spacing of 40 feet was selected for DH 23 and a spacing of 25 feet was used for DH 33 and DH 34. Accordingly, the profiling results, while representing a cumulative or apparent resistivity, can demonstrate anomalies in resistance, i. e. solution cavities, that are present throughout a certain thickness or at a particular depth. Figures 3, 4, and 5 are graphs of the profiling data.

DISCUSSION

Numerous sets of theoretical, multilayer curves have been published to facilitate comparisons of field data and estimates of depth and resistivity (Tagg, 1934; Mooney and Wetzel, 1956; Roman, 1960). Use of these curves is usually dependent on knowledge or estimates of the depth and resistivity of a surficial layer so that resistivity ratios are plotted against the ratio of electrode spacing to depth. Since our purpose was to consider a water-saturated, presumably low-resistivity, single layer for isolated solution pockets with enhanced electrical conductivity (perhaps fivefold), rather than continuous layers of contrasting resistivity, a simpler, although less exact, analysis is possible. By plotting, on log-log scales, apparent resistivity versus electrode spacing (Figure 2), the general trend of a curve may be considered similar to those using ratios. Substantial variations in trend can be interpreted as changes in electrical properties at depths based on electrode spacing.

Table 3. Apparent resistivity data (profiling) along east-west and north-south axes over drill holes DH 23 (A = 40 feet), DH 33 (A = 25 feet), and DH 34 (A = 25 feet). Values are in ohms-feet. Asterisked value is of low confidence.

Hole	Distance of Array center from hole feet	East-West Electrode arrays N	S	North-South Electrode arrays E	W
DH 23	0	40	40	64	64
	15	152	44	84	48
	30	132	60	88	132
	45	60	72	140	92
	60	280	100	60	128
DH 33	0	53	53	80	80
	25	53	46	75	112
	50	9	135	120	150
	75	10	93	122	40
	100	13		14	35
	125	10		48	10
	150	15		25	22
	175	10		20	70
	200	11			20
	225	17			27
	250	19			18
	275	33			34
	300	43			
DH 34	0	22	22	22	22
	25	30	68	26	78
	50	54	60		55
	75	88	18	75	43
	100	53	46	22	165
	125	31	22		27
	150	22	16*		18
	175	23	30		
	200	21			
	225	31			
	250	22			

Mooney (1954) has discussed the problem of depth determination at length and Parasnis (1962) has presented a summary of work relating the fraction of current reaching depths related to electrode spacings. In general, estimates of the effective depth of penetration vary from A/4 to 2A, where A equals electrode spacing. In view of the high water

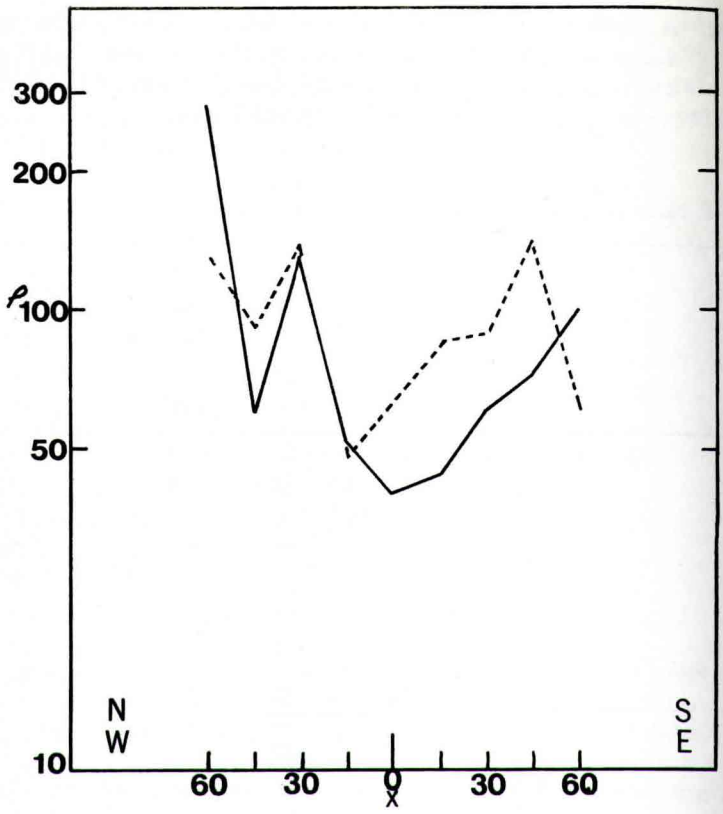

Figure 3. Apparent resistivity (ρ) in ohms-feet versus distance of array center from bore hole (X) in feet for DH 23. Electrode spacing is 40 feet. The solid line is for east-west electrode arrays arranged along a north-south grid axis and the dashed line is for north-south arrays along an east-west grid axis.

table and overall low values of resistivity recorded in this survey, we have assumed the effective depth to equal electrode spacing.

The sounding results for DH 23 (Figure 2) demonstrate an initial general increase in resistivity with electrode spacing, and therefore depth, for arrays oriented both north-south and east-west. The apparent resistivity peaks at approximately 30-40 feet, then drops sharply, suggesting the presence below that depth of a low resistance solution cavity. This is corroborated by the coring results indicating a void between the depths of 38 feet and 45 feet. The resistivity high overlying the solution cavity can not be correlated to a more resistant zone, but a general pattern of low resistance bounded by sharp high

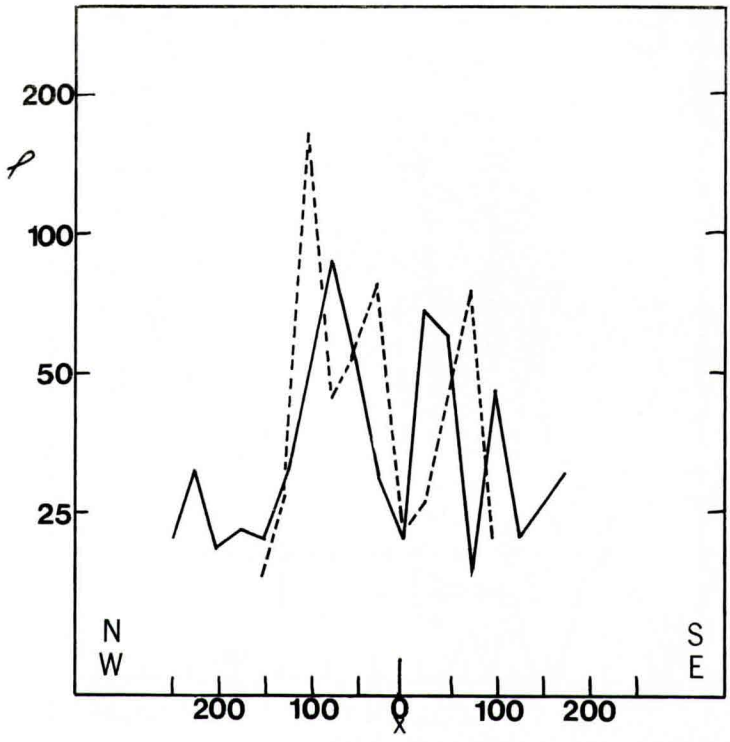

Figure 4. Apparent resistivity (ρ) in ohms-feet versus distance of array center from hole (X) in feet for DH 34. Electrode spacing is 25 feet. The solid line is for east-west electrode arrays arranged along a north-south grid axis and the dashed line is for north-south arrays along an east-west grid axis.

resistance has been theorized by Cook and Van Nostrand (1954) for filled sinks.

The log-log plots of sounding data for DH 34 (Figure 2) each show an initial decrease of apparent resistivity, followed by a slight increase, and then a sharp decrease from about 15 to 25 feet depth. The higher values (at A = 5 feet) probably represent a strong influence from the undersaturated fill material, an effect that is considerably dampened with electrode spacings of 10 feet or greater. Interpretation of the curve indicates a possible solution cavity between 15 and 25 feet depth, an excellent approximation considering the vague relationship of depth to electrode spacing. The actual void is between 15 and 19 feet as discovered by drilling. Furthermore, in contrast to the findings at DH 23 (Figure 2), it appears that a depth range, or bottom, for a cavity can be estimated if the feature is sufficiently shallow and is of only limited

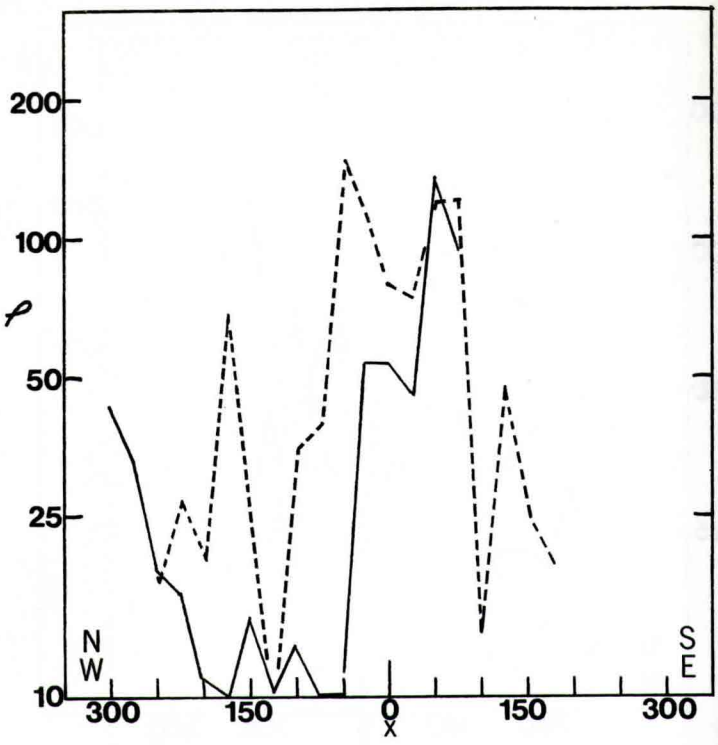

Figure 5. Apparent resistivity (ρ) in ohms-feet versus distance of array center from hole (X) in feet for DH 33. Electrode spacing is 25 feet. The solid line is for east-west electrode arrays arranged along a north-south grid axis and the dashed line is for north-south arrays along an east-west grid axis.

vertical extent.

The extent of zones of relatively low resistivity is suggested from profiling data plotted in Figures 3, 4, and 5. The graphs augment the sounding data by showing, in Figure 3, a zone of low resistivity centered perhaps slightly south and west of drill hole DH 23. Depth of consideration is presumably equal to the electrode spacing, 40 feet. Profiling data with a 25 feet electrode spacing about drill hole DH 34 (Figure 4) suggest that the low resistance zone is of limited horizontal extent and is laterally bounded by higher resistance solid material. Profiling efforts with a similar electrode spacing indicated no evidence of a solution cavity at drill hole DH 33, but an extensive cavity at about 25 feet depth is suggested about 100 feet north of DH 33 (Figures 5 and 6).

A method introduced by Moore (1945) and known as the cumulative resistivity method has been used with some success to interpret

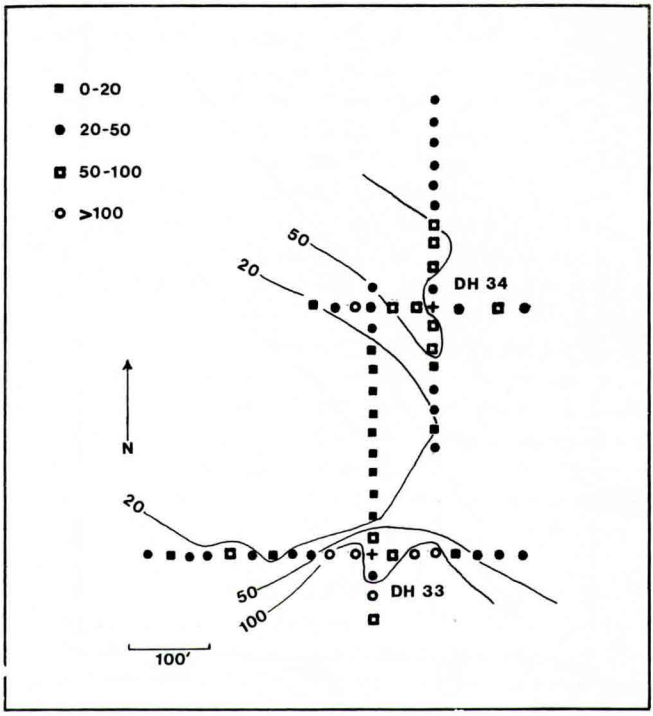

Figure 6. Contour map of profiling values (A = 25 feet) around DH 34 and DH 23. Values are in ohms-feet.

sounding data when the electrode spacing is increased by equal increments. The technique is to simply sum the total resistance for all previous electrode spacings and plot the sum for each spacing value, A. Points of slope change in the data indicate resistivity contrasts whereas linear data are interpreted as evidence of uniform resistivity. Figures 7 and 8 demonstrate applications of the Moore method to sounding data around holes DH 23 and DH 34, respectively. Both directions of arrays are plotted and average resistivities are used for the sums. The linear discontinuities on the graphs each indicate a resistivity contrast (high to low) at about 40 feet depth for DH 23 and 20 feet depth for DH 34. These results are in accord with the general interpretation of the log-log plots as verified by drilling.

CONCLUSIONS

Using the plausible assumption that solution cavities below a shallow water table are seen as a lower apparent resistivity, interpretation

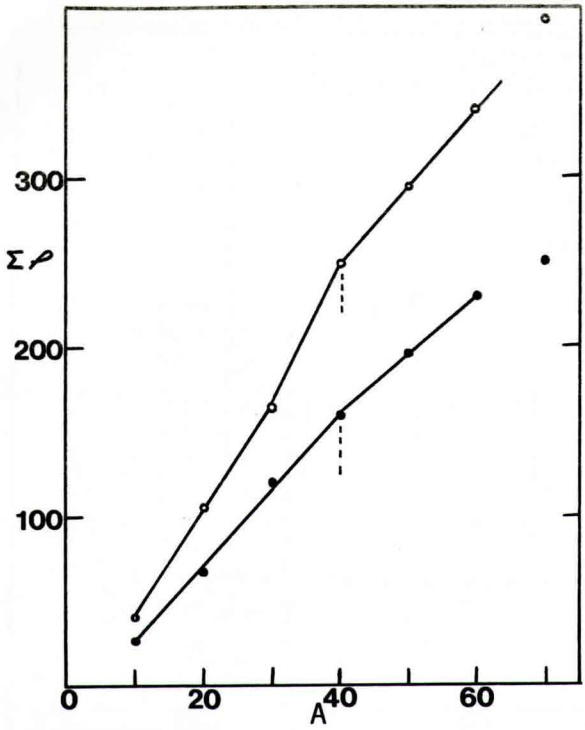

Figure 7.

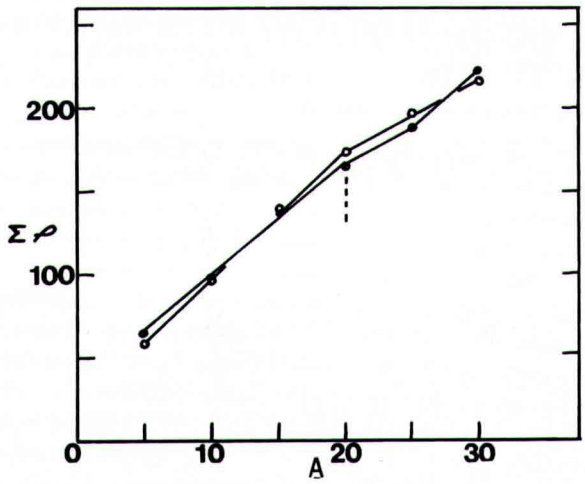

Figures 7 & 8. Moore plots of cumulative resistance ($\Sigma\rho$), in ohms-feet versus electrode spacing (A) in feet. Open circles represent data from north-south electrode arrays and closed circles indicate east-west arrays. The dashed lines denote a change to lower slope suggesting a resistivity contrast from high to low resistivity. Figure 7 refers to DH 23 and Figure 8 refers to DH 34.

of the simple and limited sounding and profiling measurements reported here is consistent with the results of drill core analyses. A solution cavity of unknown thickness at about 40 feet depth at DH 23 and a limited 5-10 feet thick cavity at about 15-20 feet depth at DH 34 are suggested on the basis of general inspection of the data graphs. These results are substantiated by the existance of cavities demonstrated by a drilling program. In addition, lateral extent of the solution cavities is suggested from profiling data. The presence of an extensive, but shallow, cavity is suggested near, but not below, DH 33 where drilling encountered no voids.

It seems apparent that simple resistivity measurements requiring uncomplicated interpretation can be used to survey the type of featureless, essentially homogeneous, karst terrain that is characteristic of north and central Florida. The potential of this inexpensive method as a preliminary tool in efficiently planning limited drilling programs for the detection of shallow solution-filled voids appears significant.

REFERENCES

Bates, E. R., 1973, Detection of subsurface cavities: U. S. Army Engineer Waterways Experiment Station Misc. Paper S-73-40, 63 p.

Bristow, C. M., 1966, A new graphical resistivity technique for detecting air-filled cavities: Studies in Speleology, v. 1, p. 204-227.

Cook, K. L., and Van Nostrand, R. G., 1954, Interpretation of resistivity data over filled sinks: Geophysics, v. 19, p. 761-790.

Dunham, R. J., 1962, Classification of carbonate rocks according to depositional texture, in Classification of carbonate rocks, Wm. Ham, Ed.: Am. Assoc. Petroleum Geologists, Mem. 1, p. 108-121.

Heiland, C. A., 1940, Geophysical exploration: Prentice-Hall, New York, 1012 p.

Jakosky, J. J., 1950, Exploration geophysics: Trija Publishing Co., Los Angeles, 1195 p.

Mooney, H. M., 1954, Depth determinations by electrical resistivity: Mining Engineering, v. 6, p. 915-918.

Mooney, H. M., and Wetzel, W. W., 1956, Potentials about a point electrode and apparent resistivity curves for a two, three, and four layer earth: Univ. of Minnesota Press, Minneapolis, 146 p.

Moore, R. W., 1945, An emperical method of interpretation of earth resistivity measurements: Trans. Amer. Inst. Min. Met. Eng., v. 164, p. 197.

Parasnis, D. S., 1962, Principles of applied geophysics: Methuen and Co. Publishers, London, 176 p.

Phillips, J. A., and Standing, I. J., 1969, The detection of caves by equi-potential surveying and electromagnetic induction location

using a tryristor pulse generator: Brit. Speleological Assoc. Proc., v. 7, p. 31-49.

Puri, H. S., and Vernon, R. O., 1964, Summary of the geology of Florida and a guide to the classical exposures: Fla. Geol. Survey, Sp. Pub. 5 (revised), 312 p.

Roman, I., 1960, Apparent resistivity of a single uniform overburden: United States Geological Survey Prof. Paper 365, 99 p.

Stringfield, V. T., and LeGrand, H. E., 1966, Hydrology of limestone terranes in the Coastal Plain of the southeastern United States: Geol. Soc. America Sp. Paper 93, 46 p.

Tagg, G. F., 1934, Interpretation of resistivity measurements: Trans. Am. Inst. Min. Met. Eng., v. 110, p. 135-147.

Textoris, D. A., Randazzo, A. F., and Thayer, P. A., 1972, Diagenesis of carbonate sediments as important non-cavern porosity controls: Proceedings 24th International Geol. Congress, Section 6, p. 190-197.

Van Nostrand, R. C., and Cook, K. L., 1966, Interpretation of resistivity data: United States Geological Survey Prof. Paper 499, 310 p.

CELESTITE IN THE MISSISSIPPIAN PENNINGTON FORMATION, CENTRAL TENNESSEE

By

William J. Frazier
Department of Earth Sciences
Columbus College
Columbus, Georgia 31907

ABSTRACT

Celestite-bearing geodes occur in the lowermost dolomicrite beds of the Pennington Formation (Upper Mississippian) along the northern Highland Rim of central Tennessee. Geodes are elliptical, up to 25 cm in length, and may coalesce. Some have brecciated margins and/or cementation-reduced central voids. Celestite occurs as small, euhedral crystals with anhydrite inclusion-rich centers. Associated with celestite is euhedral or subhedral dolomite with curved edges and undulose extinction. Other minerals associated with geodes are: quartzine, calcite, sphalerite, fluorite, and pyrite.

Based on an analogy with recent gypsum nodules and on petrographic data, Pennington geodes are interpreted as having originally formed as gypsum nodules beneath the surface of an evaporatic, sabkha-like environment, later undergoing dehydration to anhydrite. Eogenetic silicification and partial celestite replacement resulted in quartzine spherulites and inclusion-rich celestite; anhydrite later dissolved, allowing celestite to attain an euhedral shape. The source of Sr was seawater and concentration was affected by evaporation. Celestite replaces anhydrite when Ca^{++}/Sr^{++} of seawater is decreased, as for example by gypsum growth. Thus, celestite may be used as an indicator of vanished evaporites.

INTRODUCTION

The Pennington Formation (Upper Mississippian) in central Tennessee is a mixed carbonate and detrital unit consisting primarily of dolostone, shale, sandstone, and limestone. The stratigraphy and petrology have been discussed elsewhere (Frazier, 1973) and will not be mentioned here. The purpose of this paper is to describe celestite occurrences within the Pennington Formation and to discuss their origin and significance. Carbonate classification follows Folk (1959) and porosity nomenclature is that of Choquette and Pray (1970). The

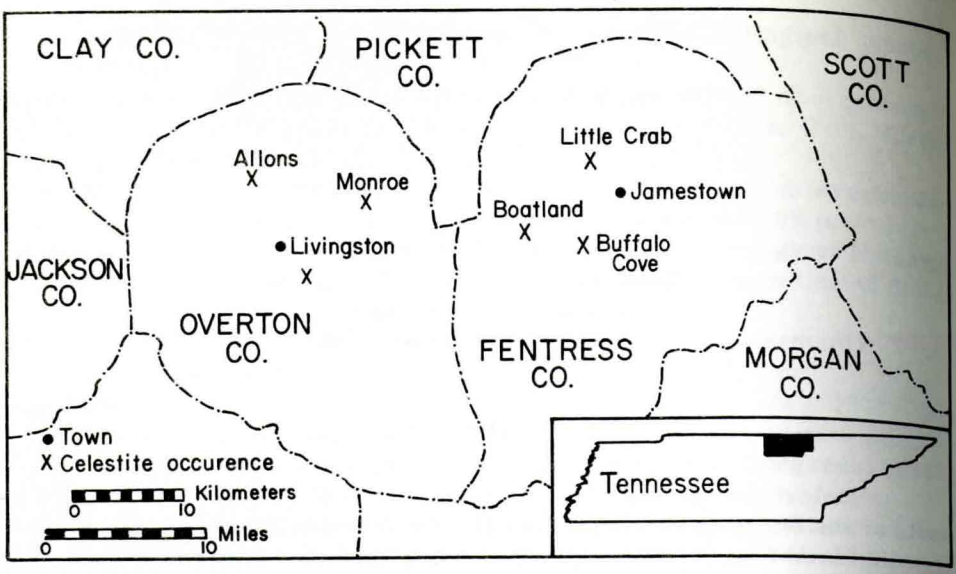

Figure 1. Map of celestite localities on the northeastern Highland Rim in Tennessee.

definition of geode proposed by Chowns and Elkins (1974) is used in this report.

Celestite ($SrSO_4$) occurs as tabular or prismatic crystals in spherical to elliptical geodes that are found both in outcrop and the subsurface along the northeastern portion of Tennessee's Highland Rim province (Figure 1). The largest concentration of celestite, at Buffalo Cove in Fentress County, was quarried for celestite between 1942 and 1944 by Inorganics, Inc., of Knoxville, Tennessee. Kesler (1944) described these occurrences at Buffalo Cove concluding that they were formed by hydrothermal activity.

Acknowledgments

This study was partially funded by the University of North Carolina Smith Fund. Daniel A. Textoris, Paul Ragland, Robert Lawrence, and Robert Milici offered assistance during the study.

DESCRIPTIONS

Country Rock

The most common lithology at the Buffalo Cove locality is dolomicrite characterized by aphanitic dolomite with rare, highly comminuted bioclasts, halite and gypsum crystal molds, and moderate amounts

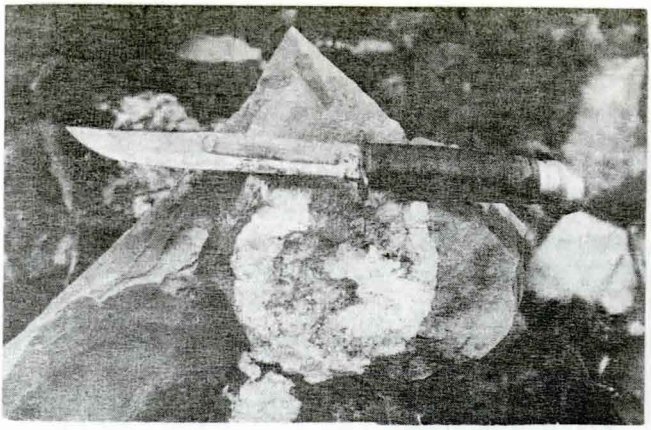

Figure 2. Typical celestite-bearing geode from Buffalo Cove, Tennessee. Notice the massive, aphanitic character of the country rock and the cementation-reduced central void with several large celestite crystals.

(10-20 percent) of clay-rich insoluble residue. Polished and etched slabs reveal vague mottling in an otherwise homogeneous, structureless rock.

Less common is partially dolomitized biomicrite. Bioclasts include abraded pelmatozoan ossicles, brachiopod valves, and bryozoan debris. The original micrite matrix has recrystallized to microspar and contains scattered dolomite euhedra.

Geodes

Most celestite-bearing geodes occur within dolomicrite a few meters above the base of the formation. The geodes are spherical to nearly flat but show a tendency to be thickly elliptical in cross-section (Figure 2), ranging in size from 1 to 25 cm. Some geodes exhibit brecciation around their margins but most have sharp, distinct borders. In some geodes, a cementation-reduced moldic void occurs in the center while in others no cavity remains. The geodes tend to occur in groups and some of them coalesce.

The paragenesis of the geodes includes (in order of abundance) dolomite, calcite, celestite, quartzine (length-slow chalcedony), sphalerite, fluorite, pyrite, and anhydrite. Dolomite occurs in several habits, the most common being large (0.2-3 cm) subhedral crystals with curved edges and undulose extinction when rotated between crossed nicols. These are usually found in geodes with cementation-reduced moldic voids. Also present are small (0.1-0.5 mm) dolomite rhombs along the margins of some geodes. Calcite occurs chiefly as subhedral

to anhedral crystals replacing both dolomite and celestite. Quartzine occurs in both geodes and country rock as small (0.5-2 mm) spherulites similar to those illustrated by Folk and Pittman (1971, Figure 11). Sphalerite and fluorite are rare and occur as euhedral crystals in central voids of geodes. Pyrite is disseminated in the country rock and anhydrite is found as inclusions in celestite crystals.

Celestite

Celestite occurs as white, blue-white, or clear crystals. Most celestite is euhedral and contains numerous inclusions of anhydrite, commonly concentrated in crystal centers (Figure 3A). Often these inclusions are arranged in such a way as to form the outline of a smaller euhedral celestite crystal in the center of a larger one (Figure 3B). In geodes that have brecciated margins, celestite occurs between the country rock fragments, often truncated by them (Figure 3C). In some geodes, anhedral celestite fills interstices between dolomite crystals (Figure 3D). Rarely, celestite is present as large, euhedral crystals in the center of geodes.

DISCUSSION

Diagenesis of Geodes

Nodules of gypsum and anhydrite with the same general size, shape, and appearance as celestite-bearing geodes from Buffalo Cove are forming today in evaporitic sediments of several areas. In the Persian Gulf, gypsum occurs as individual nodules and discontinuous layers (Illing, et al., 1965; Lucia, 1972). Anhydrite is also present on the Arabian Trucial Coast (Curtis, et al., 1963). Kerr and Thomson (1963) discussed gypsum nodules from Laguna Madre, Texas and other occurrences have been found in the sediments of the Red Sea (Degens and Ross, 1969) and of Shark Bay, Australia (Davies, 1970).

Much of the Buffalo Cove celestite contains inclusions of anhydrite, indicating that celestite originally replaced anhydrite. In addition, many geodes contain quartzine. Folk and Pittman (1971) demonstrated that the presence of quartzine is evidence for replacement of evaporitic minerals. They state, "It appears that quartzine... (characterizes) silicification is highly basic or sulphate-rich environments. Most commonly, (it occurs) in sequences of shallow marine or playa-like, evaporitic, sabkha-type deposition characterized by beds of aphanitic dolomite and nodules of gypsum, anhydrite, or rarely barite/celestite," (Folk and Pittman, 1971, p. 1056).

Chowns and Elkins (1974) describe quartz geodes from the Fort Payne and Warsaw formations of Tennessee and conclude that they are pseudomorphs after early diagenetic anhydrite nodules. They extend

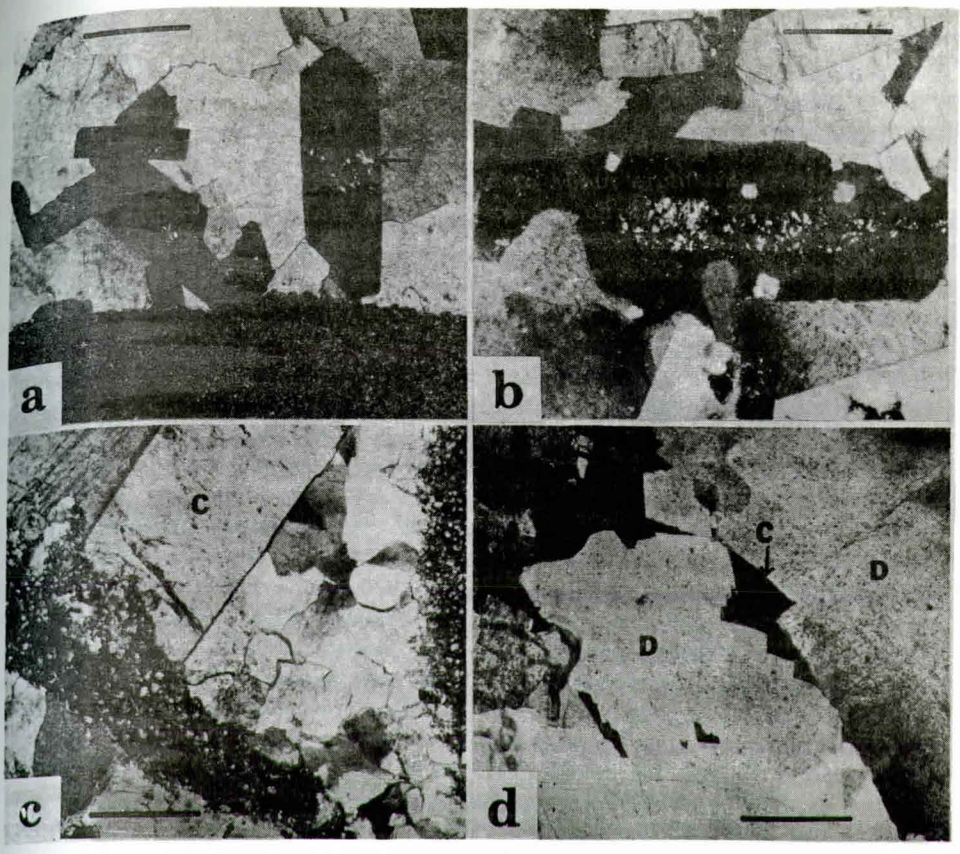

Figure 3. Thin section photomicrographs of celestite types from Buffalo Cove. A. Euhdral celestite surrounded by subhedral dolomite. Arrow indicates anhydrite inclusions. B. Euhedral celestite (at extinction) with anhydrite inclusions arranged in the center to outline a smaller euhedral celestite crystal. C. Celestite crystal (C) truncated by small rock fragment. D. Anhedral celestite (C) between subhedral dolomite (D). Notice the curved margins of dolomite crystals. All thin sections in cross nicols. Bar is 0. 5 mm.

this method of origin to geodes found in the Warsaw Formation at Keokuk, Iowa and in the Borden and Harrodsburg Formations of Kentucky and Indiana.

Based on analogy with recent gypsum and anhydrite nodules and on petrographic data, I interpret the Buffalo Cove celestite-bearing geodes as having originally formed as gypsum nodules beneath the surface of an evaporitic, sabkha-like environment. At a somewhat later time, gypsum underwent dehydration to form anhydrite (Kerr and

Thomson, 1963: Murray, 1964). This change probably occurred while the sediment was still undergoing early diagenesis (Braitsch, 1971).

After formation, the nodules underwent a complex diagenetic modification. Early silicification affected quartzine replacement of some anhydrite. Celestite may also have partially replaced anhydrite during this early stage. At a later time, anhydrite dissolved, possibly due to an increase in porewater acidity (Garrels and Christ, 1965) or to a decrease in temperature (anhydrite having a negative temperature coefficient of solubility, Weast, 1970). Since celestite is less soluble (0.135 gm/l at 25°C), than anhydrite (2.125 gm/l at 25°C), celestite crystals that had partially replaced anhydrite would remain after anhydrite dissolution. Celestite then continued to grow, resulting in euhedral crystals with anhydrite inclusion-rich centers and inclusion-free margins. Enfacial angles between some celestite crystals (Figure 3A) is evidence that this later stage of growth took place in a void (Bathurst, 1971, p. 423).

After initial growth of celestite within voids, dolomite grew as subhedral crystals with curved edges and undulose extinction, a habit interpreted as resulting from unrestricted growth into a void. Enfacial angles between dolomite crystals support this interpretation. Celestite filled intercrystalline pores between dolomite crystals, probably growing penecontemporaneously with dolomite formation. During mesogenesis, calcite replaced some dolomite and celestite. Sphalerite and fluorite probably also formed at this time.

Origin of Celestite

The source of Sr for Buffalo Cove celestite was seawater. In modern oceans, seawater contains 8 mg/l Sr (Mason, 1966). If one agrees with Rubey (1951) that the composition of seawater has changed little since earliest geologic time, it can be assumed that roughly the same amount was available in late Mississippian time.

Much of the celestite formed by replacement of anhydrite. The replacement reaction is:

$$CaSO_4 + Sr^{++} \rightleftharpoons Ca^{++} + SrSO_4.$$

The equilibrium constant (K) of this reaction is:

$$K = \frac{(Ca^{++})}{(Sr^{++})} = \frac{Ksp\ a}{Ksp\ c} = \frac{10^{-4.5}}{10^{-6.5}} = 10^2$$

where (Ca^{++}) and (Sr^{++}) are the molar concentrations of Ca and Sr and Ksp a and Ksp c are the solubility product constants of anhydrite and celestite. Thus, at ordinary temperatures, anhydrite should be replaced by celestite if it is in contact with a solution containing Sr^{++} in a concentration greater than 1/100 that of Ca^{++}.

The Ca^{++}/Sr^{++} ratio of normal seawater is 110 which is very close to the above equilibrium ratio. Any mechanism which preferentially removes Ca^{++} from seawater or seawater-derived brines would decrease the ratio and thus favor celestite replacement of anhydrite. The early diagenetic formation of gypsum and anhydrite is such a mechanism and thus carries with it the means of its own celestite replacement. Since Ca^{++} and Sr^{++} are divalent ions (and hence have the same activity coefficients), variations in the ionic strength of seawater, as would be produced by evaporation, would not effect the equilibrium ratio of the above reactions.

Deer, Howie, and Zussman (1966) state that celestite is most commonly found in vugs (or nodules) in dolostones and dolomitic limestones associated with gypsum, anhydrite, halite, and barite. West (1973) says that the presence of celestite is "a positive indication of the former presence of calcium sulphate.... " (p. 278). Since the formation of gypsum (or anhydrite) carries with it the mechanism of its own partial replacement by celestite as outlined above, the author agrees with West (1973) that celestite can provide reliable evidence for the recognition of vanished evaporites and thus aid in reconstruction of paleoenvironments and in delineation of diagenetic history.

REFERENCES

Bathurst, R. G. C., 1971, Carbonate sediments and their diagenesis: Elsevier Publishing Company, Amsterdam, 620 p.

Braitsch, O., 1971, Salt deposits: Their Origin and Composition: Springer-Verlag, New York, N. Y., 300 p.

Choquette, P. W. and Pray, L. C., 1970, Geologic nomenclature and classification of porosity in sedimentary carbonates: Am. Assoc. Petroleum Geol. Bull., v. 54, p. 207-250.

Chowns, T. M. and Elkins, J. E., 1974, The origin of quartz geodes and cauliflower cherts through the silicification of anhydrite nodules: Jour. Sedimentary Petrology, v. 44, p. 885-903.

Curtis, R., Evans, G., Kinsman, D. J. J., and Shearman, D. J., 1963, Association of dolomite and anhydrite in the Recent sediments of the Persian Gulf: Nature, v. 197, p. 679-680.

Davies, G. R., 1970, Algal-laminated sediments, Gladstone Embayment, Shark Bay, Western Australia: in Logan, B. W., Davies, G. R., Read, J. F., and Cebulski, D. E., (eds.), Carbonate Sedimentation and Environments, Shark Bay, Western Australia, Am. Assoc. Petroleum Geol. Memoir 13, p. 169-205.

Deer, W. A., Howie, R. A., and Zussman, J., 1966, An introduction to the rock-forming minerals: John Wiley and Sons, Inc., New York, N. Y., 528 p.

Degens, E. T. and Ross, D. A., 1969, Hot brines and recent heavy metal deposits in the Red Sea: Springer-Verlag, New York,

N. Y., 600 p.

Folk, R. L., 1959, Practical petrographic classification of limestones: Am. Assoc. Petroleum Geol. Bull., v. 43, p. 1-38.

Folk, R. L., and Pittman, J. S., 1971, Length-slow chalcedony: a new testament for vanished evaporites: Jour. Sedimentary Petrology, v. 41, p. 1045-1058.

Frazier, W. J., 1973, Carbonate Petrology of the Mississippian Pennington Formation, Central Tennessee: unpub. Ph. D. dissertation, University of North Carolina, Chapel Hill, N. C., 102 p.

Garrels, R. M. and Christ, C. L., 1965, Solutions, minerals, and equilibria: Harper and Row, New York, N. Y., 450 p.

Illing, L. B., Wells, A. J., and Taylor, J. C. M., 1965, Penecontemporary dolomite in the Persian Gulf: in Pray, L. C. and Murray, R. C., (eds.), Dolomitization and Limestone Diagenesis: A Symposium, Soc. Econ. Paleontologists and Mineralogists, Spec. Pub. 13, p. 89-111.

Kerr, S. D. and Thomson, A., 1963, Origin of nodular and bedded anhydrite in Permian shelf sediments, Texas and New Mexico: Am. Assoc. Petroleum Geol. Bull., v. 47, p. 1726-1732.

Kesler, T. L., 1944, Celestite in Buffalo Cove, Fentress County, Tennessee: Economic Geology, v. 39, p. 287-306.

Lucia, F. J., 1972, Recognition of evaporite-carbonate shoreline sedimentation: in Rigby, J. K. and Hamblin, W. K. (eds.), Recognition of Ancient Sedimentary Environments, Soc. Econ. Paleontologists and Mineralogists, Spec. Pub. 16, p. 160-191.

Mason, Brian, 1966, Principles of Geochemistry, John Wiley and Sons, Inc., New York, N. Y., 305 p.

Murray, R. C., 1964, Origin and diagenesis of gypsum and anhydrite: Jour. Sedimentary Petrology, v. 34, p. 512-523.

Rubey, W. W., 1951, Geologic history of sea water: Geol. Soc. America Bull., v. 62, p. 1111-1147.

Weast, R. C., 1970, Handbook of chemistry and physics: The Chemical Rubber Company, Cleveland, Ohio 2343 p.

West, Ian, 1973, Vanished evaporites - significance of strontium minerals: Jour. Sed. Petrology, v. 43, p. 278-279.

THE RARE INADUNATE CRINOID GENUS THALAMOCRINUS

By

H. L. Strimple
Department of Geology
The University of Iowa
Iowa City, Iowa 52242

ABSTRACT

The exclusively North American crinoid genus Thalamocrinus, of Silurian age, is discussed. T. ovatus and T. cylindricus are reported as coexisting in the Beech River Member, Brownsport Formation at two different exposures in Tennessee. It is noted the slightly younger (from "Linden beds") T. elongatus is also present in the upper portion of the Henryhouse Formation of southern Oklahoma. Unusually thick cup plates and an almost solid infrabasal circlet are reported for the genus indicating the cup was in contact with the sea floor rather than held above the floor by an erect stem.

The genus Thalamocrinus Miller and Gurley, 1895, is a small inadunate crinoid known only from Silurian rocks of Decatur and Benton Counties of Tennessee and Pontotoc County, Oklahoma. It is listed by Moore, Lane and Strimple in Moore and Strimple (1973, p. 18) in the family Sphaerocrinidae Jaekel, 1895, superfamily Gasterocomacea Roemer, 1854, suborder Cyathocrinina Bather, 1899, order Cladida Moore and Laudon, 1943. It is found associated with equally diminutive but prolific pisocrinids. Four species of Thalamocrinus are known at this time and are discussed below.

There are three species of Thalamocrinus known from the Beech River Member, Brownsport Formation, Ludlovian, Silurian of Decatur County, Tennessee which are T. ovatus Miller and Gurley (1895), T. cylindricus Miller and Gurley (1895) and T. globosus Springer (1926). Locality data are at best obscure for the type material so that some doubt existed as to their occurrence in the same horizon. Over a period of four years my wife Christina and myself have collected 16 specimens from two glades which are in close proximity and are the same horizon, that is, at Mt. Lebanon Church and a few miles to the east at the "Lampterocrinus glade." Most of our specimens came from the glade at Mt. Lebanon Church. T. ovatus is by far the most common and is readily distinguished from T. cylindricus which has a long slender cup with very tall basals. There are no transitional forms. We did

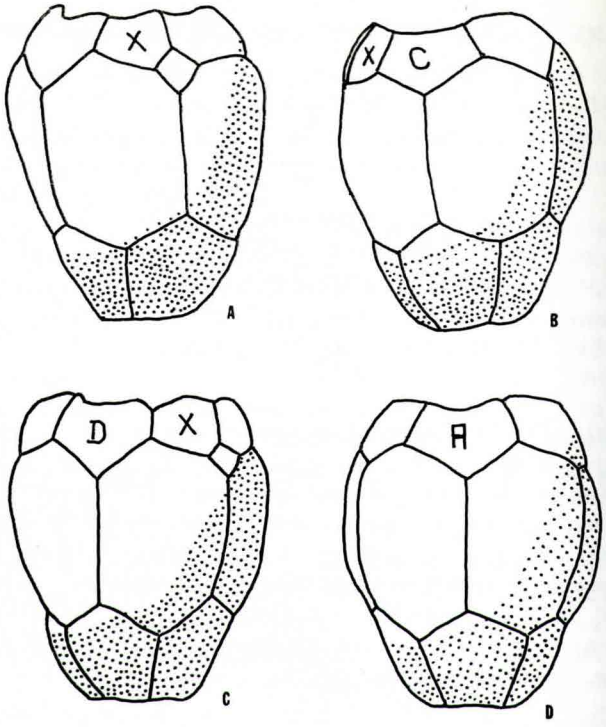

Figure 1. Camera lucida drawings of Thalamocrinus ovatus from Tennessee, hypotype SUI 38782, X12.
A-D. Cup from posterior (CD interray), C ray, D ray and anterior (A ray). Anal X identified when visible.

not recover any specimens referable to T. globosus which species has a globose shape as the name indicates.

One interesting discovery is that two specimens of T. ovatus (e. g. , Fig. 2g) have either resorbed or failed to form a radianal which is thought to represent portentum, that is, a condition within a species population representing a morphologic feature found in related species or genera at a later time. In this instance it may be observed the radianal is proportionately very small in the stratigraphically younger T. elongatus Springer (1926), indicating the element is in process of being atrophied. T. elongatus appears to be closely related to T. cylindricus from which it differs in having a broad base and a large stem.

T. elongatus was reported by Springer (ibid.) from "Linden beds, Helderbergian; near Camden, Benton County, Tennessee" which is a locality I have never visited. The "Linden beds" are currently thought

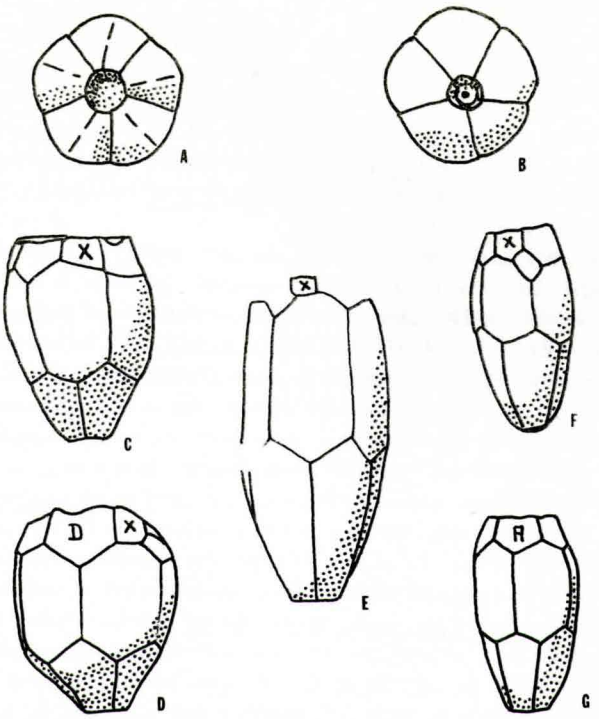

Figure 2. Camera lucida drawings of Thalamocrinus from Tennessee, X6.

A, B. Infrabasal circlet of T. ovatus, from summit and base, SUI 37783.

C. Hypotype cup of T. ovatus in which radianal is missing, SUI 38784.

D. Hypotype cup of T. ovatus viewed from D ray, SUI 38786.

E. Large hypotype of T. cylindricus with radial plates missing, viewed from CD interray, SUI 38785.

F, G. Hypotype cup of T. cylindricus viewed from CD interray and A ray, SUI 38787.

to be divided with the lower half in the Decatur Formation (Upper Silurian) and the upper half in the Lower Devonian. Without explanation Bassler and Moodey (1943, p. 708) list T. elongatus as "Sil. (Niagaran-Beech River fm.): Decatur Co., Tenn." Strimple (1963, p. 66) reported the species from the upper portion of the Henryhouse Formation (Ludlovian, Upper Silurian) of Oklahoma which is thought to be slightly younger than the Brownsport Formation (Upper Silurian) and thus indicates that Springer's specimen (the holotype by monotypy) is Silurian rather than

Devonian in age, albeit younger than Brownsport.

A specimen illustrated by Springer (ibid., pl. 26, fig. 6) as an "unusually large specimen" of T. cylindricus has a pentagonal radianal followed above by a right tube plate (RX) and therefore does not belong to the genus Thalamocrinus. Even if the RX plate was absent I would question its identification as T. cylindricus based on the shorter infrabasals and the cup outline.

The one and only basal circlet of T. ovatus found discloses a feature held in common with several genera thought to be bottom dwellers, which is the almost solid structure of the circlet. A vertical view (Figure 2e) of the circlet illustrates the solid plates reaching almost to the impressed central area. Presence of a columnal cicatrix, with presumption of an attached stem, does not negate the possibility of the base of the cup resting in a soft matrix which condition is considered by this writer to be rather common. If a long stem is present (no columnals have been observed attached to Thalamocrinus) the proximal portion is also buried, but probably sharply flexed so that the major distal portion lies on the ooze of the sea bottom. An example of a monocyclic inadunate crinoid which has developed a solid base is given by Strimple (1975) for Sygcaulocrinus typus Ulrich from Middle Ordovician rocks of Iowa, for which a bottom dwelling habitat is also postulated. The most striking example of solid infrabasals are afforded by the stemless dicyclic inadunate crinoid genera Agassizocrinus of Chesterian age. There can be no contention about these latter two genera resting on a soft bottom with the narrow base embedded in the mud. There is also no reason to suppose that any of the forms were not able to change their dwelling place at will just as the modern comatulid is known to do with the aid of their arms.

Most Paleozoic crinoids are thought to have utilized their stems to hold the crowns (cups and arms) well above the sea floor.

CONCLUSIONS

It has been confirmed that two discrete species of Thalamocrinus, T. cylindricus and T. ovatus, were coexistent in the Beech River Member, Brownsport Formation, Silurian of Tennessee at two exposures. A trend toward elimination, by resorption or abortion of the radianal plate in the lineage is demonstrated. Formation of an almost solid cup base is illustrated which is considered to reflect a bottom-dwelling habitat for the genus.

REFERENCES CITED

Bassler, R. S. and Moodey, M. W., 1943, Bibliographic and fauna index of Paleozoic Pelmatozoan Echinoderms: Geol. Soc. Amer.

Special Paper 45, 733 p.

Miller, S. A. and Gurley, W. F. E., 1895, New and interesting species of Paleozoic fossils: Ill. State Mus. Nat. Hist., Bull. 7, 89 p.

Moore, R. C., Lane, N. G., and Strimple, H. L. in Moore and Strimple, 1973, Lower Pennsylvanian (Morrowan) crinoids from Arkansas, Oklahoma and Texas, Univ. Kans., Paleont. Contr. Art. 60, 84 p.

Springer, Frank, 1926, American Silurian crinoids: Smithsonian Inst. Publ. 2871, 239 p.

Strimple, H. L., 1963, Crinoids of the Hunton Group (Devonian-Silurian) of Oklahoma: Okla. Geol. Surv. Bull. 100, 169 p.

_____, 1975, The crinoid genus Sygcaulocrinus from Iowa: Proc. Iowa Acad. Sci., v. 81, p. 116-118.